Salomon Honkala

GLONASS Satellite Navigation Signal Implementation in a Software-defined Multi-constellation Satellite Navigation Receiver

School of Electrical Engineering

Thesis submitted for examination for the degree of Master of Science in Technology.

Espoo 14.3.2016

Thesis supervisor:

Prof. Jaan Praks

Thesis advisor:

D.Sc. (Tech.) Mohammad Zahidul H. Bhuiyan

Aalto University
School of Electrical
Engineering

AALTO UNIVERSITY
SCHOOL OF ELECTRICAL ENGINEERING

ABSTRACT OF THE
MASTER'S THESIS

Author: Salomon Honkala		
Title: GLONASS Satellite Navigation Signal Implementation in a Software-defined Multi-constellation Satellite Navigation Receiver		
Date: 14.3.2016	Language: English	Number of pages: 8+51
Department of Radio Science and Technology		
Professorship: Space science and technology		Code: S-92
Supervisor: Prof. Jaan Praks		
Advisor: D.Sc. (Tech.) Mohammad Zahidul H. Bhuiyan		

Global navigation satellite systems (GNSS) provide accurate positioning, navigation and timing anywhere on Earth. Several nations have developed their own systems. The most commonly used navigation satellite system is the Global Positioning System (GPS) provided for global use by the United States. The GLONASS system is the Russian counterpart of GPS. Other systems in development are the European Galileo and the Chinese BeiDou systems.

The combined use of multiple GNSS offers many potential benefits, including improved availability, accuracy, reliability, and integrity. The use of software-defined GNSS receivers has been the focus of growing interest due to the ease of development of signal processing algorithms in software as compared to hardware. The software-defined GNSS receiver FGI-GSRx, which is used in this work, is a multi-constellation, multi-frequency software-defined receiver developed by the Finnish Geospatial Research Institute. It is a post-processing receiver developed in Matlab, currently capable of utilizing GPS, Galileo and BeiDou. This thesis presents implementation of a receiver software for the GLONASS satellite navigation system signal as part of the FGI-GSRx multi-constellation software-defined receiver. The implementation is limited to the GLONASS Standard Positioning Service signal on the L1 frequency. The implemented receiver is able to process digitized GLONASS signal samples and calculate a positioning solution. The work includes design, development, implementation, and verification of the receiver software.

Verification results show that the receiver is able to acquire and track GLONASS signals and to use them to produce a combined GPS/GLONASS positioning solution. In addition, the receiver is used to test the impact of a GPS jammer on multi-GNSS positioning, showing results of the robustness benefits of adding multiple GNSS systems to into the positioning process.

Keywords: GNSS, GLONASS, satellite navigation

AALTO-YLIOPISTO
SÄHKÖTEKNIIKAN KORKEAKOULU

DIPLOMITYÖN
TIIVISTELMÄ

Tekijä: Salomon Honkala

Työn nimi: GLONASS-satelliittipaikannussignaalin toteutus monijärjestelmä-ohjelmistosatelliittipaikannusvastaanottimessa

Päivämäärä: 14.3.2016 Kieli: Englanti Sivumäärä: 8+51

Radiotieteen ja -tekniikan laitos

Professuuri: Avaruustiede ja -tekniikka Koodi: S-92

Valvoja: Prof. Jaan Praks

Ohjaaja: TkT Mohammad Zahidul H. Bhuiyan

Satelliittinavigointijärjestelmät (GNSS) mahdollistavat tarkkoja paikannus-, navigointi- ja ajoituspalveluita kaikkialla maapallolla. Yleisimmin käytetty satelliittinavigointijärjestelmä on Yhdysvaltojen Global Positioning System (GPS). GLONASS-järjestelmä on Venäjän vastine GPS:lle. Muita järjestelmiä ovat EU:n Galileo ja Kiinan BeiDou.

Useiden satelliittijärjestelmien yhteiskäyttö tarjoaa monia mahdollisia etuja, kuten parempi saatavuus, tarkkuus ja luotettavuus. Ohjelmistomääriteltyihin GNSS-vastaanottimiin on kohdistunut kasvavaa kiinnostusta johtuen signaalinkäsittelyalgoritmien kehityksen helppoudesta ohjelmistoissa verrattuna laitteistoon.

Tässä työssä käytettävä GNSS-vastaanotin, FGI-GSRx, on ohjelmistomääritelty monijärjestelmä-monitaajuussatelliittinavigointivastaanotin, joka on kehitetty Maanmittauslaitoksen Paikkatietokeskuksessa. Se on jälkikäsittelyvastaanotin, joka tällä hetkellä pystyy hyödyntämään GPS:n, Galileon ja BeiDoun signaaleja. Työssä esitellään GLONASS -satelliittinavigointijärjestelmän signaalin vastaanoton toteutus FGI-GSRx -ohjelmistovastaanottimeen.

Toteutus rajoittuu GLONASS Standard Positioning Service -signaaliin L1-taajuudella. Lopullinen vastaanotin pystyy käsittelemään digitoituja GLONASS-signaalinäytteitä ja laskemaan paikannusratkaisun niiden avulla. Työhön kuuluu vastaanottimen ohjelmiston suunnittelu, kehittäminen, toteuttaminen ja toiminnan testaaminen.

Kokeelliset tulokset osoittavat, että vastaanotin pystyy vastaanottamaan GLONASS-signaaleja ja käyttämään niitä tuottamaan yhdistetyn GPS / GLONASS paikannusratkaisun. Lisäksi testataan häirintäsignaalin vaikutus useaa satelliittijärjestelmää hyödyntävän GNSS-vastaanottimen paikannukseen ja todetaan usean järjestelmän lisäämisen hyödyt paikannuksen häirinnänkestävyyteen.

Avainsanat: GNSS, GLONASS, satelliittipaikannus

Preface

This research was conducted within the project *Finland's Enhanced Navigation using COMPASS/BeiDou Signals* (FinCOMPASS). The project was funded by the Finnish Technology Agency (TEKES) along with the Finnish Geospatial Research Institute (FGI), Microsoft Corporation, Roger-GPS Ltd., and Vaisala Ltd. during September, 2014 till March, 2015.

I wish to thank my instructor, Dr. Zahidul Bhuiyan, for his valuable contributions and assistance. Thanks go also to my supervisor, Prof. Jaan Praks, for advice and support during the completion of this thesis. Special thanks to Prof. Heidi Kuusniemi, for giving the initiative and opportunity to complete this thesis while working at the FGI's Department of Navigation and Positioning. Thanks are also due to all of my coworkers at FGI for creating a great working environment. Finally, many heartfelt thanks to my family and friends, and especially to Jessica, for being always by my side during my studies.

Masala, 29.2.2016

Salomon Honkala

Contents

Symbols and abbreviations

Symbols

a_e	semi-major axis of Earth ≈ 6378 km
c	speed of light in a vacuum $\approx 3 \times 10^8$ m/s
C/N_0	carrier-to-noise density ratio
$\mathbf{H}$	linear connection matrix
J_2^0	second zonal harmonic coefficient of the geopotential
T_{coh}	coherent integration time
f_{IF}	intermediate frequency
t_u	receiver clock bias
$\mathbf{x}$	vector of unknown user state
$\mathbf{x}_0$	nominal state estimate vector
ε	pseudorange error
μ	standard gravitational parameter
ρ	pseudorange [m]
σ_{UERE}^2	user equivalent range error
ϕ	phase offset
ω_e	Earth rotation rate

Abbreviations

A/D	Analog-to-digital
AGC	Automatic gain control
ASIC	Application-specific integrated circuit
BPSK	Binary phase-shift keying
C/A	Coarse/Acquisition
CDMA	Code division multiple access
CGCS 2000	China Geodetic Coordinate System 2000
DFT	Discrete Fourier transform
DLL	Delay-locked loop
DOP	Dilution of precision
DSP	Digital signal processor
DSSS	Direct sequence spread spectrum
ECEF	Earth-centered, Earth-fixed
FDMA	Frequency division multiple access
FFT	Fast Fourier transform
FLL	Frequency-locked loop
FPGA	Field-programmable gate array
GNSS	Global navigation satellite system
GPS	Global Positioning System
I&D	Integrate and dump
ICD	Interface control document
IF	Intermediate frequency
ITRF	International terrestrial reference frame
LOS	Line-of-sight
LSE	Least squares estimation
MEO	Medium Earth orbit
NCO	Numerically controlled oscillator
PDOP	Position dilution of precision
PLL	Phase-locked loop
PPS	Precise positioning service
PRN	Pseudorandom noise
PZ-90	Parametry Zemli 1990
RF	Radio frequency
RMS	Root mean square
SDR	Software-defined radio
SPS	Standard positioning service
ToA	Time of arrival
UERE	User-equivalent range error
UT1	Universal Time
UTC	Coordinated Universal Time
WGS 84	World Geodetic System 1984

1 Introduction

In the last 15 years, global navigation satellite systems (GNSS) have become an extremely important part of the global infrastructure, as they enable accurate positioning, navigation and timing anywhere on Earth. Today, there are nearly four billion GNSS receivers in the world [1]. GNSS provides users with uninterrupted positioning service globally, free of charge.

The term 'GNSS' refers to a system of satellites orbiting the Earth that provides signals which can be used for navigation globally. At present, four independent GNSSs have been developed, of which two are still under development. GNSS originated as a military technology. The first navigation satellite system widely adopted for civilian use was the United States' Global Positioning System (GPS). The GLONASS system is the Russian counterpart of GPS and is nowadays used alongside GPS in multi-constellation receivers. Both the European Galileo system and the Chinese BeiDou system are currently in the deployment phase and are expected to fully complete their satellite constellations by 2020. As the operational systems will contain between 24 and 30 satellites each [2], by the end of this decade, these four GNSSs will provide more than 100 navigation satellites in total.

The increased number of satellites offers many benefits, including improved availability of navigation signals, especially in challenging environments, such as urban areas. In addition, the abundance of signals allows the receiver to select the most powerful signals, thus potentially improving accuracy. Furthermore, having multiple independent navigation signal sources yields better reliability, since a malfunction or interference in one GNSS may be detected more easily when the receiver simultaneously tracks many GNSS signals. In the near future, when BeiDou and Galileo reach global coverage, an emerging market can be foreseen for multi-constellation receivers incorporating all four systems [1].

Much research has applied GNSS receivers implemented entirely in software to experiment with multi-constellation receivers (e.g. [3], [4]). Traditionally, GNSS receivers have been based on application-specific integrated circuit (ASIC) technology [2]. The use of software defined radio (SDR) for GNSS has been the focus of growing interest due to the ease of developing signal processing algorithms in software as compared to hardware. In an SDR, the received signal is digitized as close to the antenna as possible and processed by a programmable microprocessor [5]. These software-defined receivers have been found to be a useful tool in system design and prototyping, as well as developing novel algorithms and techniques for signal processing and navigation.

Various software-defined receivers have been developed for different computing platforms and programming languages, as will be shown in Chapter 2. One such receiver is FGI-GSRx, a multi-constellation, multi-frequency software-defined receiver. It is a post-processing receiver developed in Matlab, used to process GNSS signal samples digitized using an SDR front-end. The software is currently capable of utilizing GPS, Galileo and BeiDou. However, the receiver has not been extended to use GLONASS, which has had a colorful history but has been fully deployed since 2011 [6]. Including GLONASS capability into the receiver would enhance its ability to fully take advantage of the benefits of multi-constellation GNSS.

Therefore, the aim of this thesis is to develop and implement the GLONASS signal processing parts of the FGI-GSRx software-defined receiver that would enable GLONASS transmissions to be processed and used with any combination of GPS, Galileo and/or BeiDou in order to produce a multi-constellation positioning solution. The software should process the digitized signal samples and generate the observations required to calculate the positioning solution within the framework of the FGI-GSRx. The implementation is limited to the GLONASS Standard Positioning Service signal on the L1 frequency band. The other GLONASS signals, including the L2 frequency band, encrypted Precise Positioning Service, and new L3 signals are beyond the scope of this thesis.

The remainder of this thesis is structured as follows. Chapter 2 presents the background of this work, including the fundamentals of GNSS, the tasks and operations of a general GNSS receiver, and examples of software GNSS receivers. Chapter 3 summarizes the structure and properties of the GLONASS system and navigation signal. Chapter 4 describes the implementation of the GLONASS L1-compatible multi-GNSS receiver. Chapter 5 presents the results of verification and evaluation tests done on the receiver, and conclusions are drawn in Chapter 6.

2 Satellite navigation

This chapter introduces the operating principles of GNSS, outlines the general functions of GNSS receivers and presents some developments in applications of software-defined radio techniques in GNSS. Section 2.1 describes the common principles of positioning using satellite navigation systems. Section 2.2 focuses on GNSS receivers and Section 2.3 presents several software GNSS receiver implementations as well as their applications.

2.1 Position determination

GNSS allows users to accurately locate themselves anywhere on Earth. Although several satellite navigation systems have been deployed, they all rely on the same basic principles of positioning using signals transmitted by Earth-orbiting satellites. These principles are introduced in this section.

GNSS utilizes trilateration as a positioning technique. Trilateration is the method of determining a position by measuring the distances to three known points (in this case, satellites). Navigation satellites broadcast a signal that includes ephemeris data containing information about the satellite orbit that is used to determine its position at any given time. The distance to a satellite is measured by time-of-arrival (ToA) ranging, a method of determining the distance between a transmitter and a receiver from the propagation delay of a signal [7].

The propagation delay is determined by comparing the signal transmit time to a receiver reference clock. GNSS satellites carry very precise atomic clocks. The signal broadcast by the satellites contains a time stamp, thus enabling the receiver to determine the transmit time. The propagation delay is multiplied by the speed of light c to obtain the range. Three range measurements would be enough to solve for the three-dimensional coordinates of the receiver. However, the receiver clock is inevitably out of synchronization with the GNSS system time by an unknown amount, commonly referred to as receiver clock bias. Since the clock bias, t_u, is another unknown variable to account for, in addition to the position coordinates (x, y, z), a system of equations with four unknowns is formed. An additional range measurement is needed to solve for the position and clock bias. Therefore, a minimum of four satellites are needed for successful positioning. The range measurements that include time biases are referred to as pseudoranges [7].

The pseudorange ρ_j relates the position of satellite j and receiver position according to the equation

$$\rho_j = \sqrt{(x_j - x_R)^2 + (y_j - y_R)^2 + (z_j - z_R)^2} + ct_u + \varepsilon, \tag{1}$$

where (x_j, y_j, z_j) are the coordinates of satellite j and (x_R, y_R, z_R) the coordinates of the receiver, and t_u is the receiver clock bias. ε contains all other error sources. The error sources contained in ε include measurement noise and biases, such as propagation effects and satellite clock errors, some of which can be mitigated using correction parameters transmitted by the satellites [7], [8].

Equation 1 can be linearized about a nominal state estimate, $\mathbf{x}_0 = [x_0, y_0, z_0, t_{u0}]^T$. The true position and clock bias is considered as a vector sum of the approximate estimate $\mathbf{x}_0$ and an incremental component:

$$\mathbf{x} = \mathbf{x}_0 + \Delta\mathbf{x}, \tag{2}$$

where

$$\Delta\mathbf{x} = \begin{bmatrix} \Delta x \\ \Delta y \\ \Delta z \\ -c\Delta t_u \end{bmatrix} \tag{3}$$

denotes the difference between the true receiver position and clock bias and the linearization point.

Linearizing the observation equation using a Taylor series [7], and representing the pseudorange as

$$\Delta\rho_j = \rho_{0j} - \rho_j, \tag{4}$$

where ρ_{0j} is the predicted pseudorange and ρ_j is the actually measured pseudorange, $\Delta\rho_j$ can be solved with respect to the displacement $\Delta\mathbf{x}$ by inserting Eq. (2) and (4) into Eq. (1) to yield the following:

$$\Delta\rho_j = a_{xj}\Delta x + a_{yj}\Delta y + a_{zj}\Delta z - c, \Delta t_u, \tag{5}$$

where

$$\begin{aligned} a_{xj} &= \frac{x_j - x_0}{\|\mathbf{r}_j - \mathbf{r}_0\|}, \\ a_{yj} &= \frac{y_j - y_0}{\|\mathbf{r}_j - \mathbf{r}_0\|}, \\ a_{zj} &= \frac{z_j - z_0}{\|\mathbf{r}_j - \mathbf{r}_0\|}, \end{aligned}$$

$\mathbf{r}_j = [x_j \ y_j \ z_j]^T$ denotes the coordinates of the satellite j, and $\mathbf{r}_0 = [x_0 \ y_0 \ z_0]^T$ refers to the estimated receiver position. Therefore the elements a_{xj}, a_{yj}, and a_{zj} are the direction cosines of a unit vector pointing from the receiver position to the satellite j [7].

The unknown four-element vector $\Delta\mathbf{x}$ can be solved using measurements to four satellites. A set of linear equations is formed, which can be expressed in matrix form as:

$$\Delta\boldsymbol{\rho} = \mathbf{H}\Delta\mathbf{x}, \tag{6}$$

where $\mathbf{H}$ denotes a linear connection matrix

$$\mathbf{H} = \begin{bmatrix} a_{x1} & a_{y1} & a_{z1} & 1 \\ a_{x2} & a_{y2} & a_{z2} & 1 \\ \vdots & \vdots & \vdots & \vdots \\ a_{xn} & a_{yn} & a_{zn} & 1 \end{bmatrix}, \tag{7}$$

and $\Delta\boldsymbol{\rho} = [\Delta\rho_1, \Delta\rho_2, ..., \Delta\rho_n]^T$ where n is the number of measurements available. Eq. (6) has the solution

$$\Delta\mathbf{x} = \mathbf{H}^{-1}\Delta\boldsymbol{\rho} \tag{8}$$

in the case of $n = 4$. More than four measurements can be used to minimize the effect of errors contained in ε, resulting in an overdetermined set of equations. Least squares estimation (LSE) [7] can be used, resulting in the solution as follows:

$$\Delta\mathbf{x} = (\mathbf{H}^T\mathbf{H})^{-1}\mathbf{H}^T\Delta\boldsymbol{\rho}. \tag{9}$$

The solution error covariance is [7]

$$cov(d\mathbf{x}) = (\mathbf{H}^T\mathbf{H})^{-1}\sigma^2_{UERE}, \tag{10}$$

where σ^2_{UERE} denotes the user equivalent range error, a statistical measure of the effective accuracy of the pseudorange measurements [9]. The matrix

$$(\mathbf{H}^T\mathbf{H})^{-1} = \begin{bmatrix} q_{xx} & q_{xy} & q_{xz} & q_{xt} \\ q_{yx} & q_{yy} & q_{yz} & q_{yz} \\ q_{zx} & q_{zy} & q_{zz} & q_{zt} \\ q_{tx} & q_{ty} & q_{tz} & q_{tt} \end{bmatrix} \tag{11}$$

defines the dilution of precision (DOP) parameters, which are used as a measure of the user-relative satellite geometry.

The geometric dilution of precision (GDOP) can be computed as the square root of the trace of the $(\mathbf{H}^T\mathbf{H})^{-1}$ matrix [8]:

$$GDOP = \sqrt{q_{xx} + q_{yy} + q_{zz} + q_{tt}}. \tag{12}$$

GDOP represents the relation between the pseudorange measurement errors and the position solution, depending on the satellite-user geometry. Other DOP measures are in common use, such as position DOP (PDOP), horizontal DOP (HDOP), vertical DOP (VDOP), and time DOP (TDOP) [8]. These are defined in terms of the $(\mathbf{H}^T\mathbf{H})^{-1}$ matrix as:

$$PDOP = \sqrt{q_{xx} + q_{yy} + q_{zz}}, \tag{13}$$

$$HDOP = \sqrt{q_{xx} + q_{yy}}, \tag{14}$$

$$VDOP = \sqrt{q_{zz}}, \tag{15}$$

$$TDOP = \sqrt{q_{tt}}. \tag{16}$$

2.2 GNSS receivers

The objective of a GNSS receiver is to determine a position, velocity and time solution using the signals transmitted by GNSS satellites. To this end, the receiver must obtain pseudorange measurements from at least four satellites and determine the satellite positions using the ephemeris data. This section describes, in general, the functional principles of a receiver.

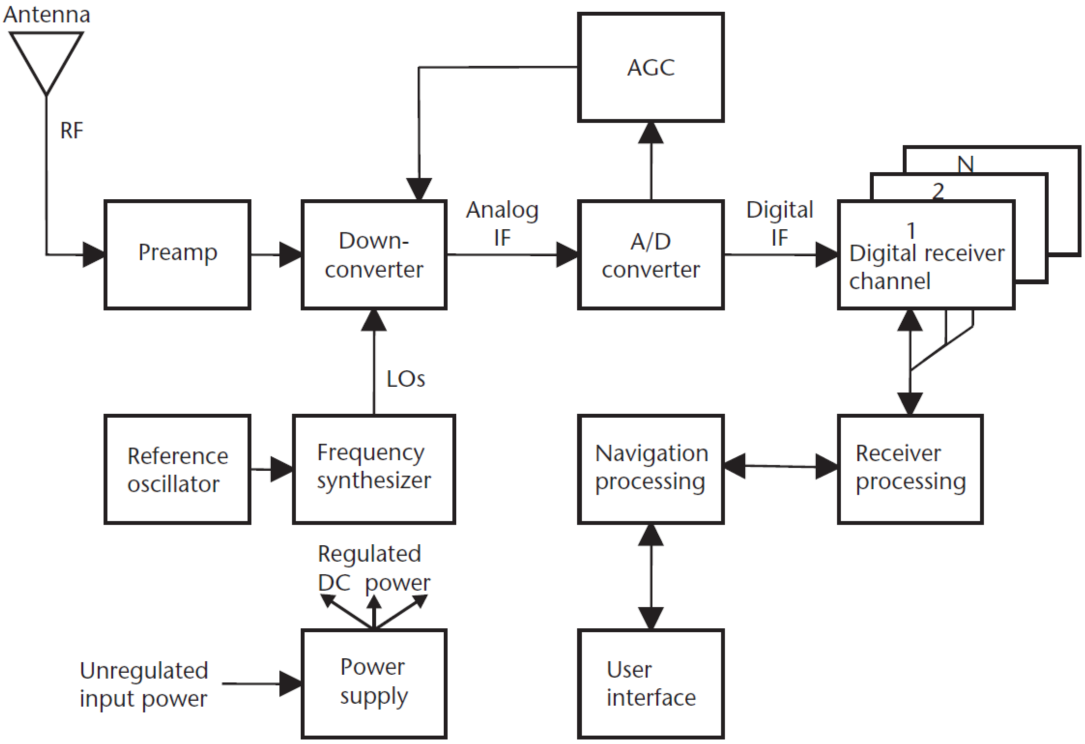

Figure 1: Block diagram of a generic GNSS receiver [10].

A block diagram of a generic GNSS receiver is shown in Fig.1. The receiver can be divided into the front-end segment and the digital processing segment. The digital processing segment usually has a number of parallel digital receiver channels, as shown in Fig. 1. The digital receiver channels are responsible for the signal processing functions, such as acquisition, tracking, and data demodulation [10]. Furthermore, the observations and data produced by the receiver channels are combined into a navigation solution by the navigation processing.

2.2.1 Front-end

The RF signal from the antenna is inserted into a front-end, which is responsible for amplification, filtering, down-conversion, and analog-to-digital (A/D) conversion. Because the received power of GNSS signals is very weak, a low-noise amplifier is typically included close to the antenna, as well as a band-pass filter to reduce out-of-band noise [10]. An automatic gain control (AGC) circuit adjusts the gain to take advantage of the full dynamic range of the A/D converter. The signal is down-converted from radio frequency (RF) to an intermediate frequency (IF), and digitized by an A/D converter.

2.2.2 Acquisition

All GNSS signals employ direct sequence spread spectrum (DSSS) modulation. A spreading code, also called the ranging code or PRN code, is used to spread a low-bit rate data signal over a wider bandwidth. The ranging code is a pseudo-random binary sequence with a wider bandwidth than the data signal it is modulating. The pulse duration of the code is referred to as a 'chip' and its frequency as the chip rate. The ranging code makes it possible to achieve precise timing synchronization between transmitter and receiver [8]. The first step in the receiver digital processing is to synchronize with the ranging code of the incoming signal.

Signal acquisition is the process of synchronizing the received GNSS signal with an internally generated local replica signal. The receiver must first detect which satellites are in view and get a coarse estimate of the carrier frequency and code phase. The signal acquisition process consists of a two-dimensional search of the carrier frequency and code phase. The search space is divided into discrete code bins and frequency bins, which divide the two-dimensional search space into cells [10].

The received carrier frequency is not precisely known due to a Doppler shift caused by the relative motion of the satellite and the receiver. In a down-conversion receiver the carrier frequency seen by the acquisition process is the IF, which is determined by the front-end oscillator frequency. Even in the IF, the Doppler shift is relative to the actual carrier frequency, and is generally within the range of ±4 kHz for a stationary user and a medium earth orbit (MEO) satellite such as GPS [7].

The phase of the ranging code in the incoming signal is at first unknown. The ranging code is a pseudo-random binary sequence that has a high autocorrelation only at zero phase difference [8]. This property allows the synchronization of the local replica of the code with the incoming code.

Acquisition techniques can be divided into time domain and frequency domain-based methods. Several time domain methods are presented in [10]. Time domain methods perform a serial search of each phase and Doppler bin by multiplication with a local replica, and integration and squaring of the result. When the signals are aligned, the resulting sum will be higher than when unaligned. Since each possible code phase value and Doppler frequency must be searched, these search methods are time-consuming. To reduce the acquisition time, parallel correlators can be used in hardware receivers to enable the simultaneous processing of multiple satellites or search bins simultanously [11].

The search of Doppler frequency or code phase can also be parallelised by incorporating a frequency domain transformation [11]. Fast Fourier transform (FFT) algorithms are used to perform the transformations, so these methods are often referred to as FFT acquisition. These methods include parallel code search and parallel Doppler search. In the parallel Doppler search, the signal is first multiplied by the local code, then Fourier-transformed and then the maximum bin of the Fourier-transform sequence is the best estimate for the Doppler frequency if the code phase is aligned. This search is repeated for each code phase, but the serial search for the Doppler frequency is eliminated. In the parallel code search, the incoming signal is first multiplied by the local replica carrier, then Fourier-transformed, then the maximum bin of the Fourier-transform is the best estimate for the code phase for each Doppler bin. Thus the need for serial code phase search is eliminated.

Without the need to search over all possible code phases, the parallel code search acquisition can be significantly faster than the serial search or the parallel Doppler search [11]. The frequency domain-based methods are well suited to software receivers, since a software receiver holds a block of the signal in memory, and it is efficient to perform the multiplications in parallel for all code phase delay values. Therefore, FFT methods allow for rapid acquisition. FFT acquisition can also acquire signals with a lower signal-to noise ratio [12].

2.2.3 Tracking

The objective of the tracking functions is to keep track of the changing Doppler effect on the carrier frequency and the phase of the ranging code as the relative velocity and range between the satellite and the receiver changes. The tracking loops "wipe off" the carrier and the ranging code modulation by mixing the incoming signal with a synchronized replica signal, so the baseband signal can be recovered.

A GNSS receiver signal tracking block is divided into carrier and code tracking loops. The objective of the carrier tracking loop is to track the GNSS signal as the carrier Doppler shift changes and remove the IF carrier from the signal, converting it to baseband. The digital IF signal is mixed with the replica IF carrier to produce the in-phase (I) and quadrature (Q) component of the signal.

For each tracking channel, the code generator in the receiver generates three replica code sequences, called early (E), prompt (P), and late (L). Typically, E is 0.5 chips ahead of P, and L is 0.5 chips delayed [10]. After carrier mixing, the I and Q signals are correlated with the early, prompt, and late replica codes, and passed through integrate-and-dump functions to produce three in-phase components, I_E, I_L, I_P and three quadrature components, Q_E, Q_L, Q_P. These signals are used as inputs to the carrier and code tracking loops. The correlation block is illustrated in Fig. 2.

2.2.4 Carrier tracking loops

The task of the carrier tracking loop is to minimize the frequency offset between the replica carrier and the incoming signal. The replica carrier is generated by a numerically controlled oscillator (NCO), which is controlled by the carrier tracking loop. A block diagram of the carrier and code loops is presented in Fig. 3. The main parts of the carrier tracking loop are predetection integrators, carrier loop discriminators, and carrier loop filters. Predetection integration refers to the integrate-and-dump processes before and within the tracking loops. The design parameters of these functions determine such performance values as carrier loop sensitivity to thermal noise and to line-of-sight dynamics as the receiver and satellites are moving [10].

Normally, the total predetection integration time cannot exceed the data bit period. The integration should not straddle a data bit transition as a sign change in the I and Q data would result in the integration result to be degraded, or totally canceled, if a sign change occurs in the middle of the integration.

The type of discriminator defines the tracking loop as a phase-locked loop (PLL), a Costas PLL, or a frequency-locked loop (FLL). A PLL is more accurate, while an

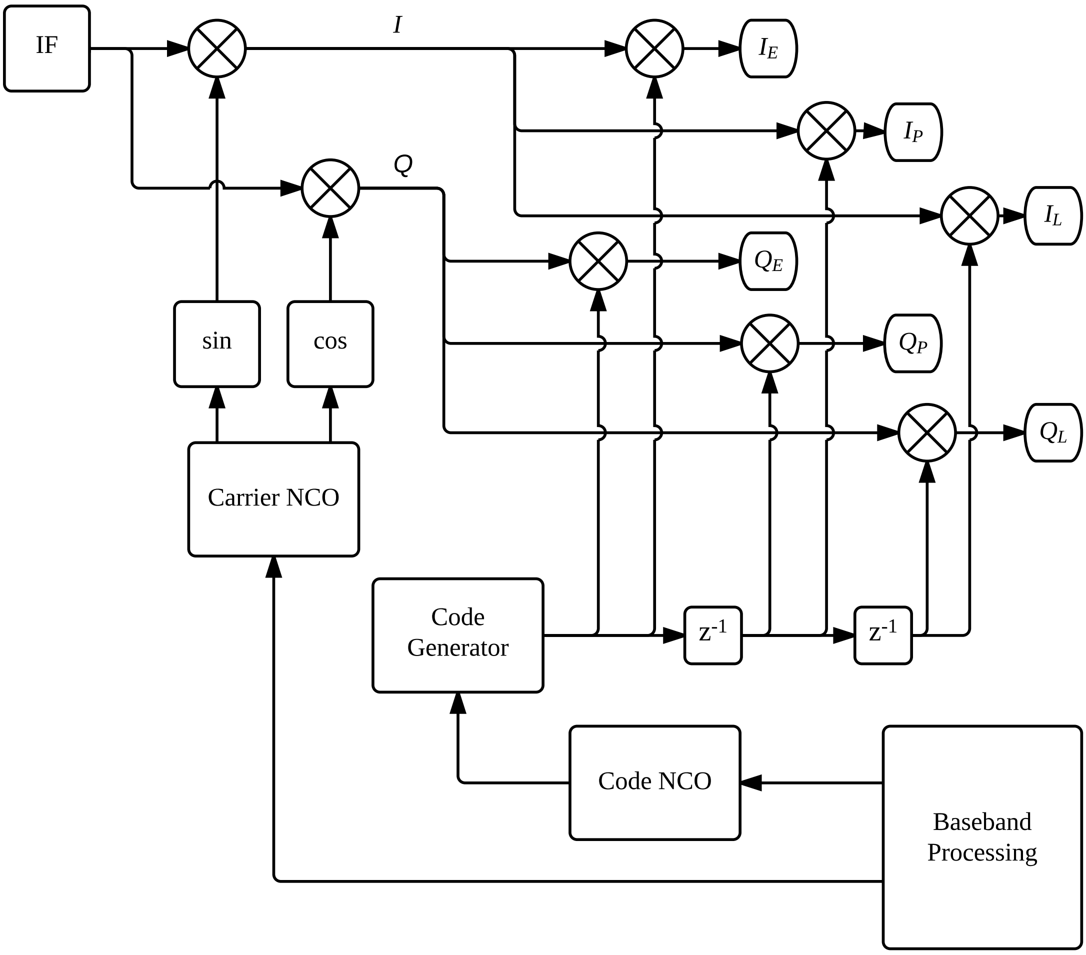

Figure 2: Block diagram of a generic digital receiver channel correlation block.

FLL is more tolerant to dynamic stress [10].

A PLL tracks the exact phase and frequency of the incoming signal. However, a pure PLL does not tolerate the 180° phase shifts associated with data modulation on the signal. A carrier loop which is insensitive to data modulation is called a Costas loop [10]. A Costas loop is used to track GNSS signals which contain data modulation. Table 1 lists several common Costas loop discriminators. The two-quadrant arctangent (ATAN) discriminator is the only one that remains linear over a range of ±90° input error, however it also has the highest computational complexity [10].

An FLL tracks the frequency of the incoming signal irrespectively of the exact phase. Common FLL discriminators are shown in Table 2. The output of the discriminators is a measure of the phase change within a sample time interval ($t_2 - t_1$), which is proportional to the frequency error in the loop. The four-quadrant arctangent ($ATAN2$) discriminator is optimal, but has the highest computational load [10]. FLLs are less sensitive to the LOS dynamics, and are therefore used initially to close in on the exact frequency before switching to PLL. Furthermore,

Table 1: Costas PLL discriminators [10].

Discriminator algorithm	Output phase error
$Q_P \times I_P$	$sin2\phi$
$Q_P \times Sign(I_P)$	$sin\phi$
Q_P/I_P	$tan\phi$
$ATAN(Q_P/I_P)$	ϕ

Table 2: FLL discriminators [10].

Discriminator algorithm	Output frequency error
$\frac{cross}{t_2-t_1}$	$\frac{sin(\phi_2-\phi_1)}{t_2-t_1}$
$\frac{cross \times Sign(dot)}{t_2-t_1}$	$\frac{sin[2(\phi_2-\phi_1)]}{t_2-t_1}$
$\frac{ATAN2(dot,cross)}{t_2-t_1}$	$\frac{\phi_2-\phi_1}{t_2-t_1}$
where: $cross = I_{P1} \times Q_{P2} + I_{P2} \times Q_{P1}$ $dot = I_{P1} \times Q_{P1} + I_{P2} \times Q_{P2}$	

an FLL-assisted PLL tracking loop is capable of automatically adjusting to dynamic stress.

2.2.5 Code tracking loops

In order to track the ranging code phase of the incoming spread-spectrum signal, a delay-locked loop (DLL) is used as the code tracking loop that aligns the local replica code with the incoming code. The code tracking loop controls an NCO which generates the base frequency of the replica code generator.

The code generator in the receiver generates three replica code sequences, called Early (E), Prompt (P), and Late (L). Typically, E is 0.5 chips ahead of P, and L is 0.5 chips delayed [10]. When the Prompt code is synchronized with the incoming signal, the magnitudes of the E and L correlation outputs equal half of the maximum correlation. Any difference between them indicates a misalignment in the code phase and the direction of the misalignment. The correlator outputs are processed by the loop discriminator to provide a quantitative measure of the code phase delay. Common DLL discriminator types are summarized in Table 3.

The carrier loop output is used to adjust the code loop output in a process called carrier-aiding of the code loop. This is done to remove the Doppler shift due to LOS dynamics from the spreading code chip rate. The carrier loop output must be adjusted by a *scale factor*, which is given by:

$$scalefactor = \frac{R_c}{f_C}, \tag{17}$$

where R_c is the spreading code chip rate, and f_C is the carrier frequency [10].

Table 3: DLL discriminators [10].

Discriminator algorithm	Description
$\frac{1}{2}\frac{E-L}{E+L}$ where: $E = \sqrt{I_E^2 + Q_E^2}$ $L = \sqrt{I_L^2 + Q_L^2}$	Noncoherent early minus late envelope normalized by $E + L$
$\frac{1}{2}(E^2 - L^2)$	Noncoherent early minus late power
$\frac{1}{2}[(I_E - I_L)I_P + (Q_E - Q_L)Q_P)]$	Quasi-coherent dot product power
$\frac{1}{2}(I_E - I_L)I_P$	Coherent dot product

2.2.6 Data demodulation

GNSS signals contain navigation data, including timing and ephemeris information, modulated on the carrier signal. In legacy signals, such as GPS Coarse/Acquisition (C/A) and GLONASS SPS, this data is modulated onto the carrier using binary phase-shift keying (BPSK) [13],[14]. BPSK is a simple signaling method where the the phase of the carrier wave is either 0° or shifted 180° depending on whether a '0' or '1' bit is being transmitted.

The data bits can be recovered when the PLL and DLL are locked and bit edge timings are known. To demodulate the BPSK signal, the I_{PS} samples are accumulated for one bit duration. The sign of the accumulated value then indicates the bit value. Due to the 180° ambiguity of the Costas PLL, the bit values may be inverted. This ambiguity can be resolved by comparing the demodulated bit sequence to a known preamble sequence contained within the data message. If the preamble is found inverted, the PLL is locked to a 180° offset and all bits will be inverted. Otherwise, if a non-inverted preamble is found, the bit stream is non-inverted.

When the the data bit duration is longer than code repetition period, the receiver does not know the timing of the data bit transitions although the code loop

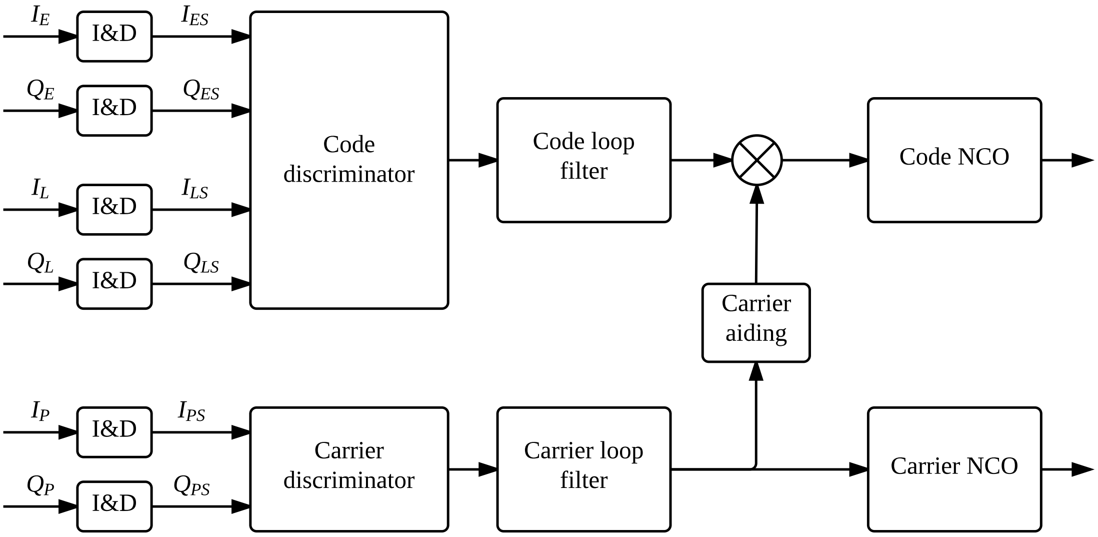

Figure 3: Block diagram of the tracking loops of a generic GNSS digital receiver channel. The discriminator inputs are produced by integrate and dump (I&D) accumulators. The correlator outputs are processed by the code and carrier tracking loop, which in turn control the replica carrier and code generators through numerically controlled oscillator (NCO) functions.

is synchronized with the incoming ranging code. In addition to preventing data demodulation, a bit transition in the middle of a predetection integration interval will cause a degraded integration result [13]. Therefore, bit edge timings must be determined by the bit synchronization process. A simple approach is to sum the prompt correlator outputs over the data bit duration at each of the possible bit edge times, and select the highest sum value to find the most probable bit edge timing [10]. Until the bit edges are located, short integration times can be used to ensure that most integration intervals do not contain a bit transition.

2.2.7 Navigation

In order to produce a positioning result, the receiver must determine the positions of the satellites at the time of transmission and determine the pseudorange to each satellite. The satellite position determination is done by using the satellite ephemeris from the data messages, which are transmitted as part of the navigation signal. The ephemeris describes the orbit of a satellite and relates the position of the satellite to time.

Determination of the pseudorange is done by using the transmit time of the data message and the receiver clock. The precise transmit time can be determined from the navigation message and the code phase of the replica code [10]. Comparing the transmit time to the receive time based on a local reference clock yields the propagation delay. The propagation delay is multiplied by the speed of light to obtain the pseudorange. The pseudorange ρ_j to satellite j is obtained from receiver time t_R and transmit time t_{Tj} using the following equation:

$$\rho_j = c(t_R - t_{Tj}) \tag{18}$$

This measurement is contaminated with bias errors in both the receiver clock and the satellite clock [10]. The receiver clock bias is eventually estimated by the navigation process as part of the navigation solution. The satellite clock offsets to the true system time are monitored and corrections are transmitted as part of the navigation message. These corrections are applied to the pseudorange measurements by the navigation process.

The pseudorange equations for each satellite are combined to form a system of nonlinear equations, with the clock bias δt_b, and the position coordinates (x_R, y_R, z_R) as unknowns. If at least four measurements are available, the system can be linearized and solved numerically by linear algebra methods, such as least squares estimation, as shown in Section 2.1. Information on the relative quality of the measurements can be combined in the solution to form a weighted least squares estimate [7]. Past solutions can be utilized in a recursive solution, which can be produced by using Kalman filtering [15].

2.3 Software GNSS receivers

A software GNSS receiver is a GNSS receiver whose digital signal processing algorithms are implemented entirely in software. This section presents current GNSS research utilizing software receivers, such as research on multi-constellation receivers, interference mitigation, fault detection and integration of GNSS with inertial navigation systems. The section includes a survey of software GNSS receivers published in the literature, and presents the FGI-GSRx software receiver.

2.3.1 Software-defined radio

Traditionally, the digital signal processing functions of GNSS receivers have been based on application-specific integrated circuit (ASIC) hardware, which enables low manufacturing cost and high performance [2]. However, the design and prototyping process is costly and time-consuming. The use of software defined radio (SDR) technology for GNSS has been the focus of growing interest in recent years. In an SDR receiver, the RF signal is digitized as close to the antenna as possible [5]. The resulting digital samples are processed by a programmable microprocessor, such as a digital signal processor (DSP) or a general-purpose processor in a PC. A variety of software GNSS receiver implementations have been developed and tested since the first GNSS software receiver [16] presented in a 1997 dissertation. However, further work is needed to address the implementation of a software receiver that supports all global navigation satellite systems (i.e., GPS, GLONASS, BeiDou, and Galileo).

Software receivers have been applied to current GNSS research topics such as multi-constellation receivers, interference mitigation, fault detection, and integration of GNSS with inertial navigation systems. Some efforts have focused on creating a fully applicable software receiver, others have used it test specific algorithms. Many of the receivers designed to process the signals in real time have achieved this by implementing the functions with the highest computational load, such as the correlators, using high-performance computation techniques such as assembly-language optimizations and single-instruction, multiple-data (SIMD) processing. Others have chosen to retain the flexibility and ease of development of high-level languages where real-time processing is not required.

2.3.2 Previous work

As mentioned above, the first GPS/GLONASS software receiver was presented in the 1997 dissertation of D. Akos [16]. This work consisted of the development of a receiver front-end hardware and Matlab signal processing and navigation software.

Some software receivers have been developed to accompany GNSS textbooks as an educational tool for illustrating the inner workings of a GNSS receiver. The SoftGNSS receiver presented by Borre et al. in [11] is a Galileo and GPS receiver written in the Matlab language. Matlab scripts are also utilized in [17] to illustrate the design of a GPS receiver. Gleason et al. [18] use FastGPS, a GPS receiver written in C++, to demonstrate many of the steps performed in a GNSS receiver. An open-source GLONASS L1 receiver written in the Scilab language has been developed based on the SoftGNSS receiver [19].

Software receivers have been used in research on GNSS signal tracking in low signal-to-noise-ratio situations or otherwise challenging environments. Reliable navigation is vital in many activities, thus considerable efforts are directed towards detecting and mitigating interference in the GNSS signal bands. This interference can be either unintentional or deliberate (i.e., jamming). For instance, the effects of out-of-band interference on GNSS receivers have been evaluated using a software receiver [20]. Since novel signal processing methods are easy to implement in software receivers, they have been used to develop methods for jamming detection [21], identification [22], and mitigation [23]. Another interference mitigation technique, using adaptive antenna arrays, has been studied using a real-time GPS/Galileo/BeiDou software receiver written in C++ and utilizing the USRP software radio platform [24].

GSNRx, a GNSS software receiver in C++ developed and maintained by the PLAN Group of the University of Calgary was developed initially for GPS, and was modified to add GLONASS [25]. Later Galileo and BeiDou signals have been added [3].

IpexSR is a real-time capable software GNSS receiver which can receive signals from GPS, Galileo and satellite-based augmentation system (SBAS) satellites [26]. The receiver was implemented in C++ and optimized through the use of assembler instructions and multi-threading. It has been used in GNSS reference stations.

The authors of [27] presented an open source hardware/software GNSS receiver, the TUTGNSS Reference Receiver, which was developed for educational and research purposes. The baseband parts of the receiver were implemented as a modular design on a field-programmable gate array (FPGA) hardware using the VHDL hardware description language. The navigation software was written in the C language.

In [4], the authors presented an open source GPS C/A and Galileo E1 software receiver, called GNSS-SDR. The software was written in C++ and is compatible with several different RF front-ends. The receiver was tested with real-life signals from the in-orbit-validation Galileo satellites.

In [28], the authors evaluated the feasibility of implementing a LabView-based, real-time platform for development and prototyping of GPS receivers. Different hardware options were compared. A software platform was described, developed by the authors utilizing C/C++ integrated with LabView.

Three GNSS receiver architectures were compared in [29], including the traditional ASIC-based hardware receiver, fully software-defined receiver, and a novel multi-core processing architecture. This work focused on possible consumer device applications. The SDR approach was seen as flexible, but challenging to achieve real-time processing. The multi-core processor was proposed to address the speed limitations, using an array of reconfigurable processors.

2.3.3 FGI-GSRx

FGI-GSRx is a software defined, multi-constellation, multi-frequency, post-processing GNSS receiver, developed by researchers at the Finnish Geospatial Research Institute (FGI), (formerly Finnish Geodetic Institute). The receiver is originally based on the SoftGNSS GPS and Galileo software receiver [11], and is intended as a research tool. FGI-GSRx is written entirely in Matlab, which makes it suitable for flexible testing of receiver design strategies and positioning algorithms.

The receiver is entirely software-defined, running in the Matlab numerical computing environment. It is a post-processing receiver where the signal is not processed simultaneously as it is received, but instead previously stored signal files can be processed. The signal is first received with a front-end which digitizes the signal. The signal is output to a a binary file and stored on a PC. This raw signal is processed by the software receiver.

The receiver is capable of processing the following navigation signals: GPS L1 C/A, BeiDou B1 [30], [31], [32] and B2 [33], Galileo E1, and the Indian regional navigation satellite system IRNSS [34]. GLONASS capability in FGI-GSRx is implemented as a part of this thesis.

3 GLONASS specifications

This chapter presents GLONASS (Russian: *Globalnaya Navigatsionnaya Sputnikova Sistema*, Global Navigation Satellite System) in detail, including the signal structure and frequency bands, and space segment, a comparison between GLONASS and other systems, and planned GLONASS modernization.

The GLONASS system began development in the Soviet Union in the 1970s as a military system. The first satellite was launched in 1982, and a full constellation of 24 satellites was reached in 1995. The satellite constellation degraded soon after as older satellites failed and could not be replaced due to lack of funding. In 2001 the Russian government initiated a 10-year program to rebuild the system [35]. A full constellation of 24 satellites was restored in 2011 [6].

GLONASS consists of three components: the constellation of satellites (space segment), ground based control facilities (control segment), and user equipment (user segment). The control segment is responsible for monitoring constellation status, determining orbital parameters, updating navigation data, and uploading control commands [14]. The user segment consists of all equipment receiving the GLONASS signal in order to provide navigation information.

3.1 Signal structure

GLONASS provides two navigation signals. The standard accuracy SPS signal is open and free to use globally. The precise accuracy PPS signal is intended for military use, and no official specifications of it have been published.

This section describes the SPS navigation signal, its frequency allocation, modulation, ranging code, and performance specifications. Information on the interface between the space segment and the user segment is published by the GLONASS authorities in the form of a GLONASS Interface Control Document (ICD) [14]. The ICD specifies all system parameters required to receive the SPS signal.

3.1.1 Frequency plan

The satellites transmit navigation signals on two frequency bands, L1, centered around 1602 MHz, and L2, centered around 1246 MHz [14]. The GLONASS L1 and L2 frequency bands are occasionally referred to as G1 and G2 to distinguish them from GPS frequency designations.

Each of the bands is shared between the satellites using frequency division multiple access (FDMA). The bands are divided into 14 channels according to the following formulas:

$$\begin{aligned} f_{K1} &= f_{01} + K\Delta f_1, \qquad & \Delta f_1 &= 562.5\ kHz \\ f_{K2} &= f_{02} + K\Delta f_2, \qquad & \Delta f_2 &= 437.5\ kHz \end{aligned}$$

where f_{01} and f_{02} are the center frequencies for each band, separation between channels is Δf_1 for L1 and Δf_2 for L2, and K is the number of the channel. The channels are numbered from -7 to 6. Each satellite is allocated a pair of carrier frequencies according to its channel number K. A summary of the channel carrier frequencies is provided in Table 4. As there are 24 satellites, but only 14 frequency channels, satellites in opposite orbital slots (antipodal satellites) can transmit on the same frequency channel [14].

Table 4: GLONASS frequency channels [14].

Channel	Frequency in L1 band, MHz	Frequency in L2 band, MHz
6	1605.3750	1248.6250
5	1604.8125	1248.1875
4	1603.2500	1247.7500
3	1603.6875	1247.3125
2	1602.1250	1246.8750
1	1602.5625	1246.4375
0	1602.0	1246.0
-1	1601.4375	1245.5625
-2	1600.8750	1245.1250
-3	1600.3125	1244.6875
-4	1599.7500	1244.2500
-5	1599.1875	1243.8125
-6	1598.6250	1243.3750
-7	1598.0625	1243.9375

3.1.2 Received power

The minimum received signal power level is specified for a satellite observed at a 5° elevation angle using a 3 dBi linearly polarized antenna to be –161 dBW for the L1 and L2 bands. At higher elevation angles, the power level can be higher, but is not expected to be more than –155.2 dBW [14].

3.1.3 Ranging code

The SPS signal ranging code is a maximum length sequence (m-sequence or MLS), which repeats every 511 bits [14]. The sequence is generated by a 9-stage shift register as shown in Fig. 4. The 9-stage shift register is described by the generating polynomial $G(x) = 1 + x^5 + x^9$. The shift register is initialized with the sequence 111111111. The code is generated by sampling at the 7th value of the shift register. The code has a chip rate of 511 kbps, and a repetition period of 1 ms. The same ranging code is used by all satellites.

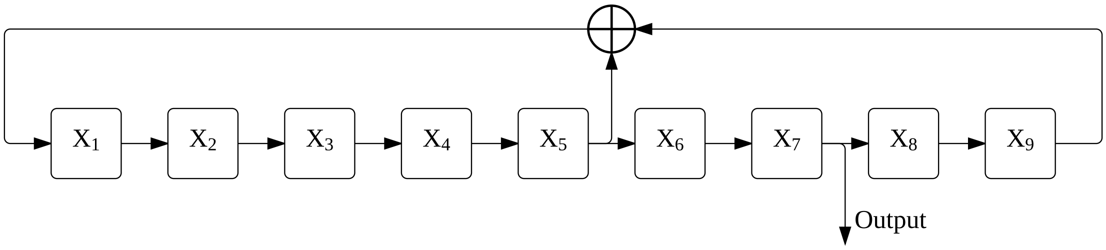

Figure 4: Structure of the feedback shift register generating the GLONASS ranging code. The feedback value is formed by modulo-2 addition of the values of the 5th and 9th registers, and the ranging code is formed from the values of the 7th register.

3.1.4 Modulation

The navigation data is encoded onto the carrier using binary phase-shift keying (BPSK) at a bit rate of 50 bits per second (bps). The signal is additionally modulated by a 100 bps auxiliary meander sequence, which ensures that there will be a bit flip in the middle of each data bit. This type of coding is referred to in the ICD [14] as bi-binary coding, and is also known as Manchester coding. The structure of the data bit encoding is illustrated in Fig. 5. In total, the sequence modulating the carrier frequency is a modulo-2 addition of the following binary sequences: the pseudorandom ranging code at 511 kbps, the navigation message at 50 bps, and the meander sequence at 100 bps [14]. Thus, the GLONASS signal can be represented as follows:

$$s(t) = \sqrt{2P}R(t)M(t)D(t)cos(2\pi ft + \phi) \tag{19}$$

where P is the signal power, $R(t)$ is the ranging code, $M(t)$ is the meander sequence, $D(t)$ is the data sequence, f is the carrier frequency, and ϕ is the phase offset.

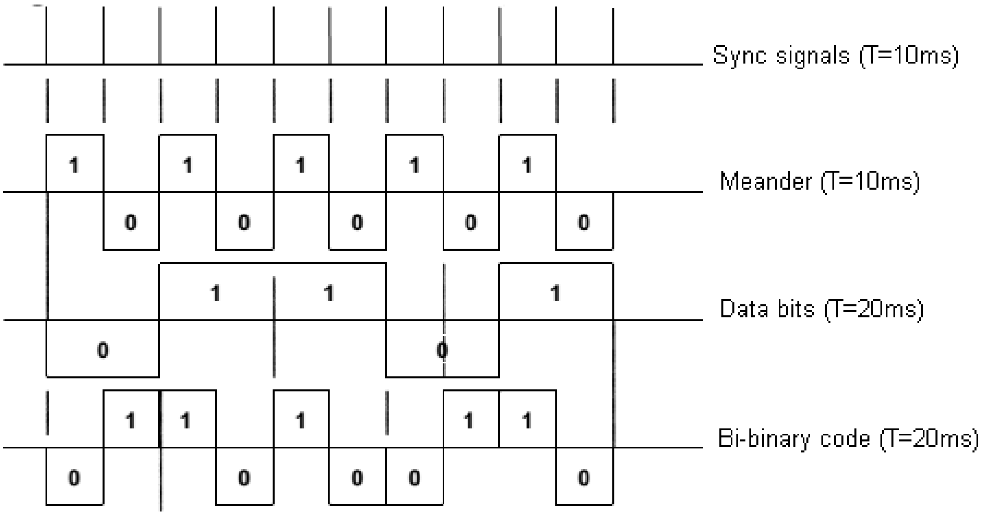

Figure 5: Encoding of the GLONASS data bits. The combination of the data bits and the meander sequence forms the bi-binary code. Figure adapted from [14].

3.2 Navigation message

The navigation data is structured as superframes that repeat every 2.5 minutes. A superframe consists of 5 frames, which have a duration of 30 seconds. Each frame consists of 15 strings of 2 seconds duration.

A string contains the data bits of the navigation message and a time mark. The 85 data bits are transmitted during the first 1.7 seconds of each string. The bits are transmitted in decreasing order (from 85 to 1). Bits 1 to 8 are error-correcting bits of a Hamming code. Bits 9 to 84 contain the data, and bit 85 is always zero. The data bit length is 20 ms. The time mark is a predetermined sequence of 30 bits with a bit length of 10 ms. The time mark is transmitted in the last 0.3 seconds of each string [14].

The navigation data message contains immediate data and non-immediate data. The immediate data includes the ephemeris parameters, clock corrections, and health information of the transmitting satellite. Additionally, the reference time of the immediate data is transmitted as the parameter τ_b. The ephemeris parameters consist of the XYZ position, velocity and acceleration coordinates of the satellite at the reference epoch τ_b. The immediate data is transmitted in strings 1 to 4 of every frame, and is constant within one superframe [14].

A part of the non-immediate data is transmitted in strings 5 to 15 of each frame, so that the total content of the data is transmitted during one superframe. The non-immediate data, or almanac, contains GLONASS system time parameters and coarse time corrections, orbital parameters, and health information of all GLONASS satellites. The orbital parameters in the non-immediate data enable a receiver to calculate the approximate positions of all GLONASS satellites. The time parameters include time offsets of GLONASS time relative to Universal Coordinated Time (UTC), Universal Time (UT1), and GPS time [14].

3.3 Reference frames

A terrestrial reference frame is a specific realization of a spatial reference system, i.e. a set of physical points with precisely determined coordinates in the reference system [7]. GNSS measurements are referenced to a specific realization of the International Terrestrial Reference System (ITRS). The international standard terrestrial reference frame is the International Terrestrial Reference Frame (ITRF), which is maintained by the International Earth Rotation and Reference Systems Service (IERS).

The coordinate reference frame used by GLONASS is the geocentric reference coordinate frame PZ-90 (*Parametry Zemli 1990*, Parameters of the Earth 1990) [14]. Since December 31, 2013, GLONASS adopted the latest version, PZ-90.11, which closely coincides with the ITRF2008 coordinate frame, as does the World Geodetic System 1984 (WGS 84) frame used by GPS [36].

The time reference of GLONASS is so-called GLONASS time, which is defined relative to UTC(SU), which is the UTC reference maintained in Russia. There is a constant three-hour offset between GLONASS time and UTC(SU):

$$T_{GLO} = T_{UTC(SU)} + 03h\ 00min$$

The error between GLONASS time and UTC(SU) should not exceed 1 microsecond [14]. The error of satellite onboard time scales to central GLONASS time should not exceed 10 ns. Transformation between onboard time t and UTC(SU) can be calculated by the following equation [14]:

$$T_{UTC(SU)} + 03h\ 00min = t + \tau_c + \tau_n(t_b) - \gamma_n(t_b)(t - t_b), \tag{20}$$

The time correction parameters τ_c, τ_n, and γ_n are given in the navigation message and referred to the epoch t_b.

3.4 Space segment

The GLONASS space segment, or constellation of satellites, is nominally composed of 24 satellites orbiting the Earth in three orbital planes, with 8 satellites in each plane [14]. The orbits are circular at altitude 19 100 km. The orbital period is 11 hours, 15 minutes and 44 seconds. The ground track repetition period is 17 orbital periods, or 7 days, 23 hours, 27 minutes and 28 seconds.

The satellites are placed in orbital slots that are numbered from 1 to 24 so that plane 1 contains slots 1–8, plane 2 slots 9–16 and plane 3 slots 17–24. The slot numbers increase backwards of the direction of satellite rotation around the Earth. The spacing between the slots in a plane is 45 degrees. The orbital planes are inclined 64.8 degrees to the equator [14].

The GLONASS satellites have evolved over three generations of satellite types: the original GLONASS design, the modified GLONASS-M, and the new GLONASS-K satellites. The original GLONASS satellites transmitted the SPS and PPS signals on the L1 band and only the PPS signal on L2, and had design lifetimes of three years [35]. GLONASS-M satellites have been launched since 2003. The GLONASS-M has a number of improvements, such as improved navigation performance, a longer lifetime of 7 years, a civil SPS signal on L2, and an improved navigation message [35]. At the time of reaching full operational capacity in 2011, the operational constellation consisted of 23 GLONASS-M satellites and one GLONASS-K [6].

3.5 Comparison of GLONASS with other GNSS

This section compares the differences between GLONASS in comparison to other current GNSSs. A summary of the differences between GLONASS, GPS, and BeiDou is provided in Table 5.

3.5.1 Signal structure

The main difference of the GLONASS signal in comparison with other systems is the FDMA multiplexing method. The other systems use code division multiple access

(CDMA). In a CDMA system, all satellites transmit on the same carrier frequency, but using different ranging codes that have such cross-correlation properties that the satellite signals can be distinguished from each other [13]. In the FDMA method used by GLONASS all satellites have their separate frequency channels and can therefore use the same ranging code. The entire GLONASS L1 band is 8 MHz wide, which demands a wider bandwidth in the receiver compared to the CDMA signals.

3.5.2 Navigation message

GLONASS transmits ephemeris information in the form a set of satellite location, velocity and acceleration vectors in three-dimensional Cartesian coordinates. Therefore calculating GLONASS orbital positions is significantly different from other current GNSSs, which all use modified Keplerian elliptical orbital parameters in their ephemeris messages.

GLONASS does not provide any ionospheric or tropospheric delay correction parameters in the navigation message. However, a multi-constellation receiver can apply the ionospheric and tropospheric models transmitted by other systems also to GLONASS.

3.5.3 Reference frames

Since GLONASS time is tied to the UTC time reference, it implements leap second corrections. Leap seconds are added to UTC usually every 1 to 1.5 years according to notification by the IERS. Each leap second adds one second to the offset between GLONASS time and GPS time, since GPS time does not add leap seconds. GPS, Galileo, and BeiDou use continuous time scales which do not implement leap seconds. The three-hour difference from UTC in GLONASS is another unique property. The other systems start their time scales from 0 h UTC.

The coordinate reference frames used in GNSSs, such as PZ-90.11, WGS 84, and China Geodetic Coordinate System (CGCS 2000) are different realizations of the same terrestrial reference system. The reference frames are therefore not identical. The transformation between PZ-90.11 and the WGS 84 have been determined to consist of a linear origin shift of some centimeters [36].

3.6 Modernization of GLONASS

The next generation of GLONASS satellites, GLONASS-K, is planned to include a new CDMA signal. The new signal is planned to enhance the interoperability with the other GNSSs.

The first GLONASS-K1 satellite was launched in 2011, and a second in 2014 [37]. The satellites are undergoing testing of the new CDMA signal on L3 band, 1207 MHz. At the time of this writing, no signal specifications for the GLONASS-K CDMA signals have been published. The planned GLONASS-K2 series satellites will transmit new civil CDMA signals on L1 and L2 bands as well [6].

Table 5: Comparison of open service signals of GLONASS, GPS, and BeiDou satellite navigation systems.

	GLONASS	GPS	BeiDou
Number of satellites	24	24	35
Orbital altitude	19 100 km	20 200 km	21 500 km
Orbital inclination	64.8°	55°	55°
Multiplexing	FDMA	CDMA	CDMA
Frequency bands	L1: 1602 MHz	L1: 1575.42 MHz	B1: 1561.098 MHz
	L2: 1246 MHz	L2: 1227.6 MHz	B2: 1207.14 MHz
	L3: 1207.14 MHz	L5: 1176.45 MHz	B3: 1268.52 MHz
Ranging code	M-sequence	Gold code	Gold code
Code chip rate	0.551 MHz	1.023 MHz	2.046 MHz
Code length (chips)	511	1023	2046
Code period	1 ms	1 ms	1 ms
Reference frame	PZ-90	WGS 84	CGCS2000

4 GLONASS L1 receiver implementation

This chapter describes the implementation of the GLONASS L1 functions in the FGI-GSRx software receiver. The functions are separated into acquisition, tracking, data demodulation, and navigation message processing for each signal type. The functional blocks of the receiver are described, reflecting the structure of Section 2.2.

The goal of developing and implementing the GLONASS signal processing part of FGI-GSRx is to enable GLONASS to be used with any combination of GPS, Galileo and/or BeiDou in order to produce a multi-constellation positioning solution. The primary outputs of this part of the receiver are the pseudorange measurements and satellite positions, which are used to calculate the positioning solution.

GLONASS capability is incorporated into the existing framework of the FGI-GSRx software-defined receiver. The receiver should be able to process the digitized GLONASS signal samples and calculate the positioning solution. The implementation is limited to the GLONASS Standard Positioning Service FDMA signal on the L1 frequency. The other GLONASS signals, including the L2 frequency, the encrypted Precise Positioning Service, and the future modernized CDMA signals are beyond the scope of this thesis.

FGI-GSRx is a fully functioning receiver for GPS, Galileo and BeiDou and all the functions are in place for these signals. GLONASS functions were developed to fit into the existing receiver structure. Parts of the software were modified to implement the GLONASS functions.

4.1 Front-end

FGI-GSRx is compatible with a number of RF front-ends, such as SiGe GN3S Sampler, NSL Stereo, and USRP. The front-end used in this work to receive the RF signals was the Stereo v.2 dual frequency front-end from Nottingham Scientific Ltd. shown in Fig. 6. It is flexibly configurable to any GNSS frequency band with a bandwidth wide enough for GLONASS, and also capable of receiving signals on two bands simultaneously. The Stereo front-end contains two RF front-end modules: a Maxim MAX2112 and a MAX2679b [38].

Table 6: Maxim 2679b front-end GLONASS configuration.

Center frequency	1602 MHz
Filter bandwidth	8 MHz
Intermediate frequency	4.62 MHz
Sampling rate	26 MHz
Data type	2-bit Real

The signal is digitized as with a configurable bit depth, using either real or complex sampling. The 2679b module provides real-valued samples, while the 2112

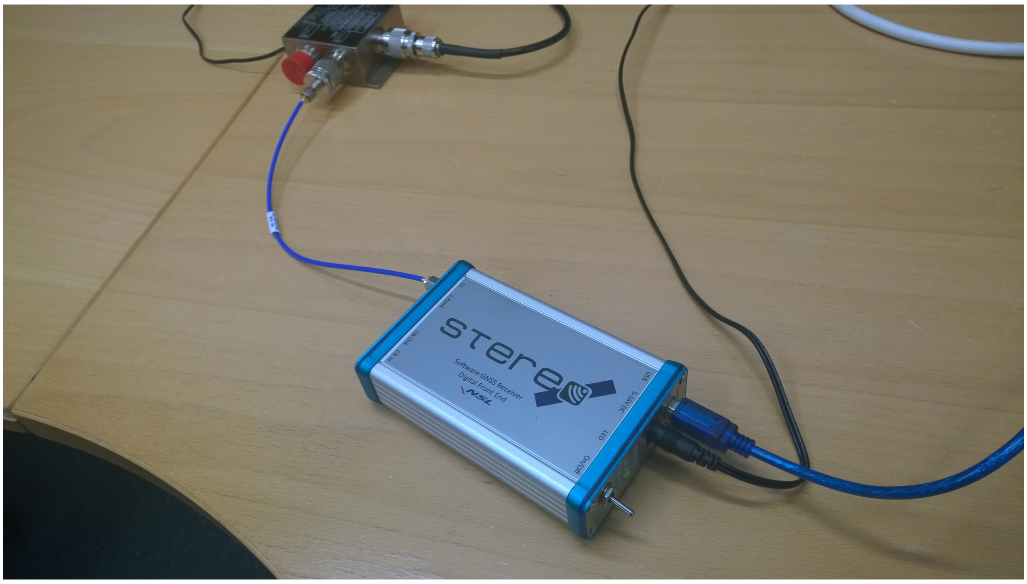

Figure 6: Stereo multi-GNSS front-end.

employs I/Q sampling, and outputs complex-valued data. The bit depth of the A/D conversion can be configured to 1, 2, 4, or 8 bits [38].

The GLONASS implementation was tested using the front-end configuration shown in Table 6. An example of the IF signal logged with this configuration is shown in Figures 7–9. Fig. 7 shows the IF spectrum of the signal filtered with an 8 MHz bandwidth, which is sufficient for the GLONASS L1 band. The GLONASS signals are not directly visible in the spectrum due to the spread spectrum signal being hidden by noise before further processing. Fig. 8 shows 0.02 ms of the signal in the time domain and Fig. 9 shows a histogram of the digitized sample values for the first 100 ms.

Once the file is stored, the IF signal can be processed by FGI-GSRx. The correct parameters, including the center frequency, intermediate frequency (f_{IF}), sampling rate, and data type, must be provided for the software receiver.

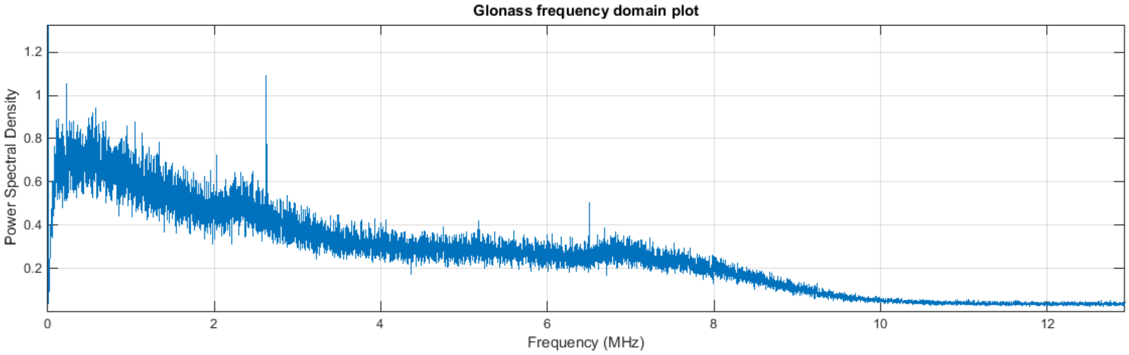

Figure 7: Power spectral density of an IF signal logged for GLONASS receiver testing.

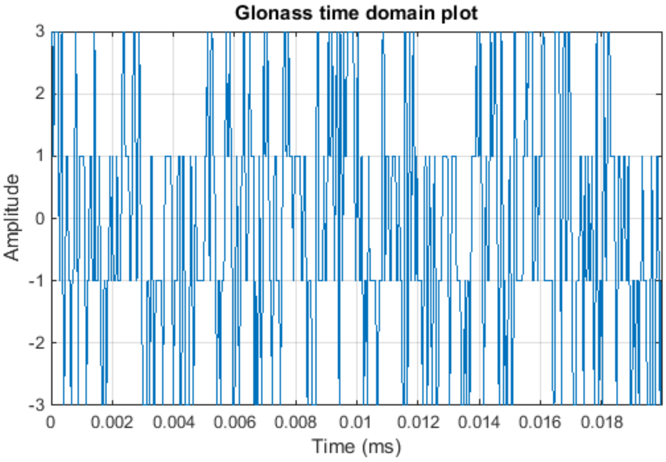

Figure 8: Amplitude values of a portion of the digitized GLONASS signal in the time-domain.

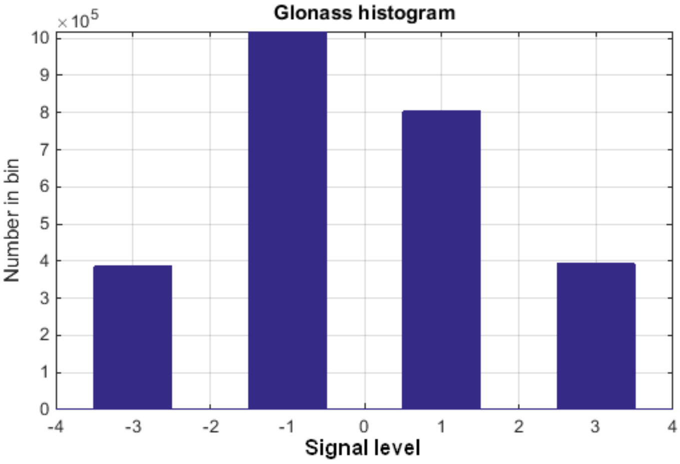

Figure 9: Histogram of the digitized GLONASS signal amplitude values over a period of 100 ms.

4.2 Acquisition

The acquisition was implemented using a parallel code acquisition technique (see section 2.2.2). The algorithm is already used for the other signals in FGI-GSRx, and the GLONASS implementation required the some modifications to be made. The GLONASS implementation differs in the code generation, as only one ranging code needs to be generated in the receiver. Also, the frequency channel of the acquired satellites must be determined, so instead of searching for every PRN code as in the GPS acquisition, the GLONASS acquisition searches for a signal on each frequency channel. The frequency channel number then becomes an additional parameter in the satellite data structure.

Since the GLONASS satellites use identical ranging codes, their slot numbers cannot be identified at the acquisition stage, whereas each GPS satellite has a unique ranging code. The GLONASS slot numbers are not available until the navigation message has been demodulated. Therefore, the GLONASS frequency channel numbers are used to label the satellites during acquisition and tracking.

Selecting longer coherent and non-coherent integration times during acquisition can improve acquisition sensitivity. For the GLONASS signal, because of the 10 ms meander code of the data modulation, there is a possibility of a bit transition boundary every 10 ms. A longer coherent integration time could cause loss of signal power as the signal will partly cancel itself out. A 5 ms coherent integration (T_{coh}) was selected after testing different settings. 5 ms was found to be a suitable value, but lower values were also found to be adequate for acquisition of 6 or more of the strongest signals.

The Doppler frequency search bandwidth was set to 14 kHz. The search band is divided into frequency bins. The size of the bins is equal to $1/(2T_{\text{coh}})$[10]. The integration result is compared to a predetermined detection threshold to determine whether a satellite signal is present or not. The optimal detection threshold depends on the integration times and bin sizes, and was selected based on test results. An example of acquisition results is presented graphically in Fig. 10. The acquisition threshold was 8 in this case. A higher value of 10 could be generally used in order to exclude the weakest signals and reduce the probability of false alarm.

In order to verify the acquisition functionality of the implemented receiver, live signals were collected using the front-end configuration described in the previous section. The antenna used was a high-grade active antenna installed on the roof of the FGI building. The acquisition results were compared with orbit predictions of GLONASS satellites.

Ten satellites were predicted to be above the horizon at the time. The acquired satellites are shown in Table 7. Nine out of the ten satellites were acquired, verifying the acquisition functionality.

The acquisition function provides the list of acquired satellites and coarse estimates of the Doppler frequencies and code phases as outputs. These outputs are used to initialize the tracking channels.

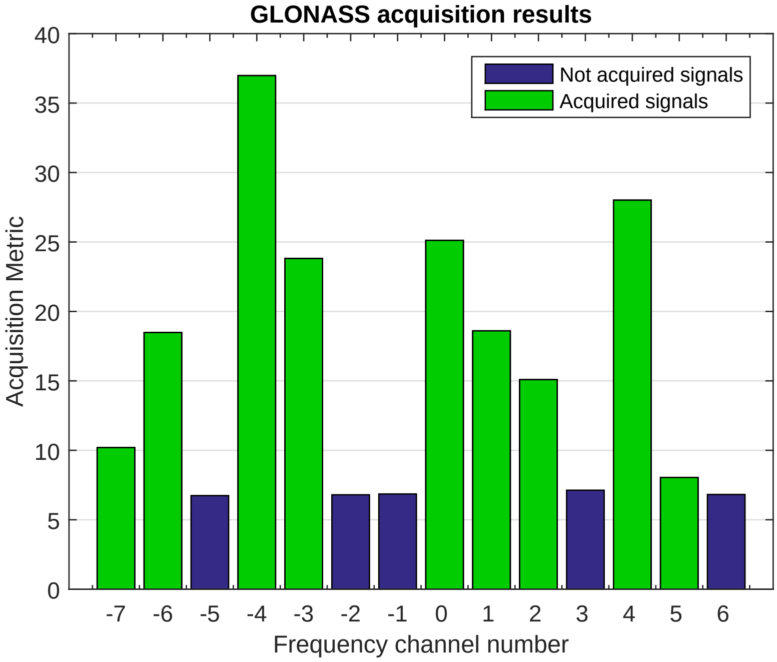

Figure 10: Acquisition results for each GLONASS frequency channel, showing acquisition metric based on integration result. A green bar indicates the metric is above the acquisition threshold.

Table 7: Acquired GLONASS L1 signals.

Slot number	Channel	Acquired
1	1	Yes
2	−4	Yes
3	5	Yes
9	−2	No
10	−7	Yes
11	0	Yes
17	4	Yes
18	−3	Yes
24	2	Yes
25	−6	Yes

4.3 Tracking

Since FGI-GSRx is a post-processing receiver, the tracking is run for the complete input signal data on all channels before beginning data demodulation. The IF signal is first transferred to baseband by the carrier tracking loop. The baseband signal is correlated the with the local replica code by the code tracking loop. The tracking functions are called once for each 1 millisecond period. The early, prompt, and late correlator outputs are assigned into vector data structures for later processing.

The tracking process outputs the I and Q components of the E, P, and L correlator values. The I_P correlator output is used later in the data demodulation and transmit time calculations.

The tracking loops track the incoming carrier frequency and code phase of each channel (see Section 2.2). The code phase is tracked by a DLL. The DLL discriminator is a noncoherent normalized early minus late envelope discriminator. The carrier frequency is tracked by an FLL-assisted PLL tracking loop. A four-quadrant arctangent discriminator is used in the FLL. A two-quadrant arctangent discriminator is used in the PLL. GLONASS versions of the tracking functions were developed for the GLONASS tracking channels, taking into account the different ranging code and the frequency multiplexing.

Each tracking channel has a carrier frequency variable determined by the Doppler frequency and the base carrier frequency of the signal, which depends on the constellation and frequency channel.

The GLONASS data bit duration is 20 ms, with a 10 ms meander ensuring a bit transition in the middle of each data bit. Therefore, a bit transition may occur

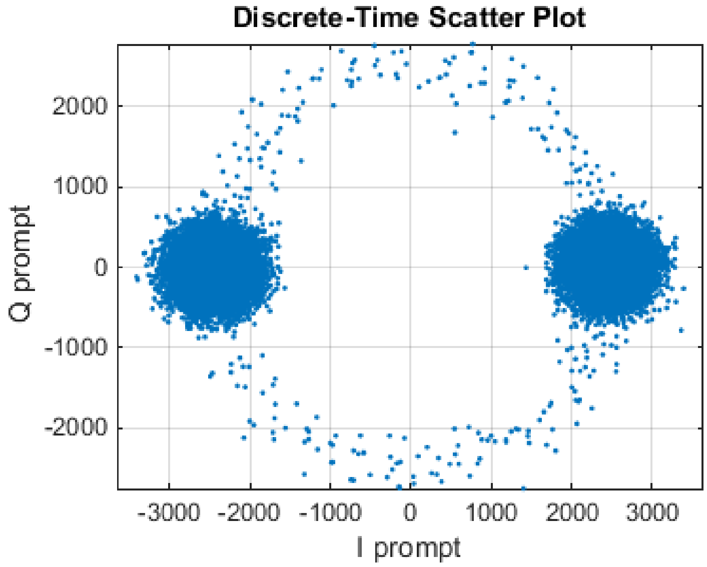

Figure 11: I/Q plot of the I_P and Q_P outputs when the PLL is locked to the carrier frequency.

every 10 ms. The bit synchronization function checks for sign changes in the I_P values. When the number of sign changes spaced at exactly 10 ms intervals reaches a threshold value, a bit synchronization is found.

In order to verify the tracking loops, and to test positioning performance, a 50 seconds long IF data set was collected with the front-end configuration shown in Table 6. The receiver needs at least 30 seconds of continuous signal to receive the navigation data needed for positioning.

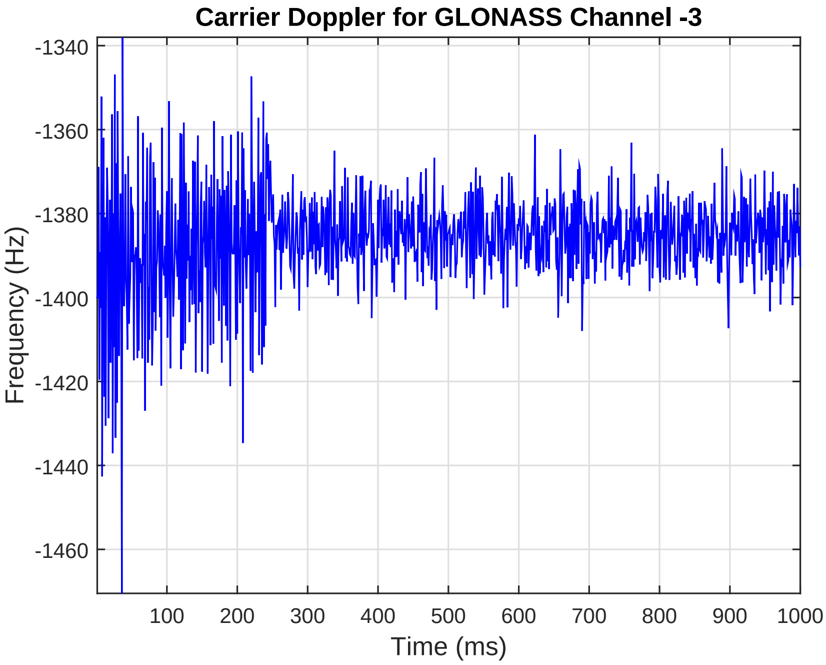

Figure 12: Doppler frequency estimate for tracked GLONASS signal on frequency channel -3.

Fig. 11 shows an I/Q scatter plot of the tracking output, showing that the signal energy is mostly contained in the I component, while the Q component is mostly noise. The I/Q scatter plot confirms that the PLL is correctly locked, tracking the carrier phase and frequency.

Fig. 12 shows the tracked Doppler frequency of one of the tracked satellites for the first second after tracking has begun. It shows that the frequency is being tracked correctly, and after bit synchronization at 250 ms, the FLL-assisted PLL transitions to PLL mode, which has a narrower noise bandwidth.

The early, prompt, and late correlator outputs used in code tracking of a GLONASS signal are shown in Fig. 13. The power of the prompt correlator is higher than the early and late, as expected when the code phase is being tracked by the DLL. The I_P and Q_P outputs are plotted in Fig. 14, where bit transitions can be seen in the I_P data.

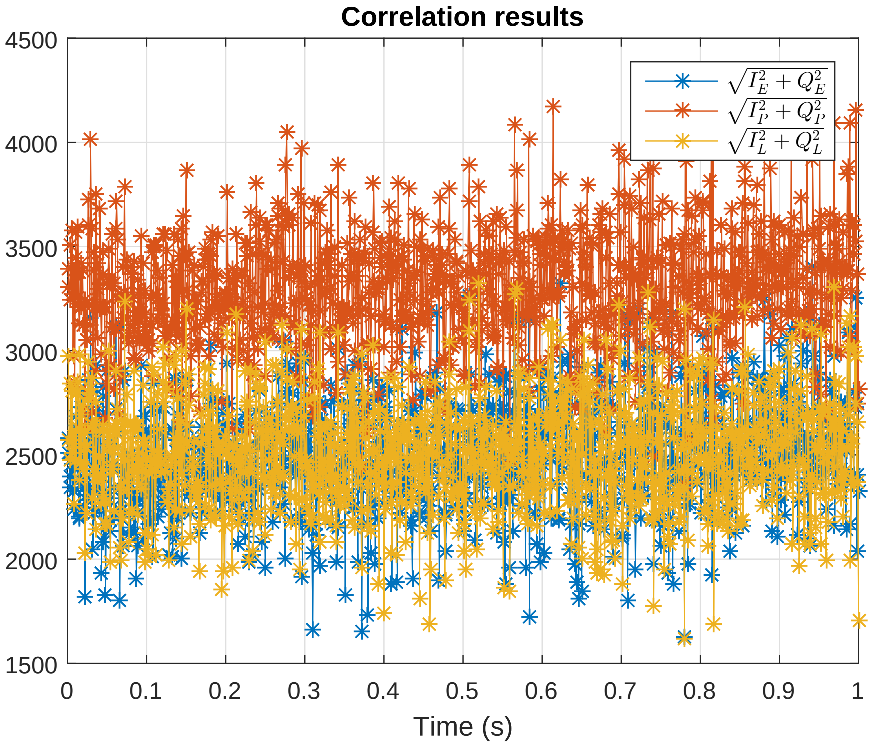

Figure 13: Early (blue), prompt (red), and late (yellow) correlators output magnitude (unitless) for tracked GLONASS signal on frequency channel -4. The prompt output is highest, as the prompt code replica is synchronized with the incoming code.

4.4 Data demodulation

Data demodulation functions search for the GLONASS time mark sequence in the I_P output stream in order to find the start of the navigation message and then decode the data.

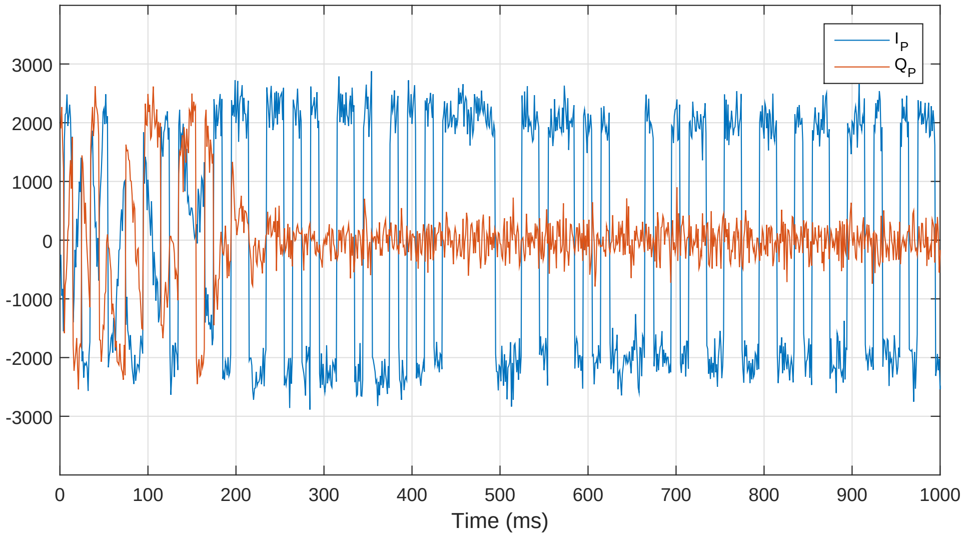

Figure 14: I_P (blue) and Q_P (red) correlator outputs (unitless). Navigation data bits are visible in I_P after 200 ms.

First the meander code is removed decoding the data into a 50-Hz bit stream. To find the beginning of the first data string, correlation is used to search for the time mark sequence. Once the time mark is found, the string is decoded according to the ICD [14], and the GLONASS ephemeris, time correction, and other satellite data are stored for later use in the navigation processing.

The data demodulation was verified by comparing the demodulated data to GLONASS broadcast ephemeris data retrieved from the International GNSS Service, which distributes GNSS observations and ephemeris data for scientific and engineering purposes (https://igscb.jpl.nasa.gov/).

4.5 Satellite positions

The GLONASS ephemeris data contains the satellite position, velocity, and acceleration in Cartesian coordinates in the ECEF coordinate frame PZ-90.11. These are the predicted coordinates at a reference epoch 15 minutes from the time when new data are transmitted. This data is updated every 30 minutes. To determine the satellite position at a specific time, the satellite trajectory is propagated forwards or backwards from the epoch using numerical integration of the differential equations that describe the motion of the satellite.

The ICD provides an example algorithm for propagating the orbit, which uses the 4th order Runge-Kutta method [14]. The force model takes into account the standard gravitational parameter of the Earth μ, the second zonal harmonic coefficient J_2^0 (polar flattening of the Earth), and the perturbations caused by lunar and solar gravitation. The accelerations caused by luni-solar perturbations, $\ddot{x}_{ls}$, $\ddot{y}_{ls}$, and $\ddot{z}_{ls}$, are retrieved from the navigation message and are assumed to be constant during the integration interval of ±15 minutes. since the satellite coordinates are defined in the ECEF coordinate frame PZ-90.11, which rotates with the Earth, the rotation of the Earth is modeled in these equations with the Earth rotation rate ω_e.

The motion of the satellite is described by the following system of differential equations:

$$\dot{X} = V_x \tag{21}$$

$$\dot{Y} = V_y \tag{22}$$

$$\dot{Z} = V_z \tag{23}$$

$$\ddot{X} = -\frac{\mu}{r^3}X + \frac{3}{2}J_2\frac{\mu a_e^2}{r^5}X(1-\frac{5Z^2}{r^2}) + \omega_e^2 X + 2\omega_e V_y + \ddot{x}_{ls} \tag{24}$$

$$\ddot{Y} = -\frac{\mu}{r^3}Y + \frac{3}{2}J_2\frac{\mu a_e^2}{r^5}Y(1-\frac{5Z^2}{r^2}) + \omega_e^2 Y - 2\omega_e V_x + \ddot{y}_{ls} \tag{25}$$

$$\ddot{Z} = -\frac{\mu}{r^3}X + \frac{3}{2}J_2\frac{\mu a_e^2}{r^5}X(3-\frac{5Z^2}{r^2}) + \ddot{z}_{ls} \tag{26}$$

where a_e is the semi-major axis of the Earth, and $r = \sqrt{X^2+Y^2+Z^2}$.

A Matlab implementation of the 4th order Runge-Kutta solution has been developed in previous work as part of a master's thesis [39]. The numerical integration of the satellite motion can also be done using a built-in Matlab function, ODE45. In a comparison of different methods for calculating GLONASS satellite coordinates [40], the ODE45 calculation has been found to be as accurate, but computationally more efficient. The ODE45 was therefore chosen as the method to be used in this work.

The satellite position solution was verified by comparing satellite positions propagated forwards from one broadcast ephemeris data to the broadcast positions in the next epoch 30 minutes later. The difference in the positions was approximately 2 m on average. This result is consistent with the mean square error of the GLONASS broadcast ephemeris, which is 7 m in the cross-track and along-track components and 1.5 m in the radial component [14].

4.6 Navigation

The positioning solution is computed by the navigation block of FGI-GSRx, using pseudorange observables and satellite positions produced by the system-specific functions. Fig. 15 shows how the GLONASS observables and satellite positions are used.

The pseudorange observables are formed by subtracting the transmission time from the current receiver time estimate. For the first loop, the receiver time estimate is initialized to a fixed offset from one of the satellite transmit times.

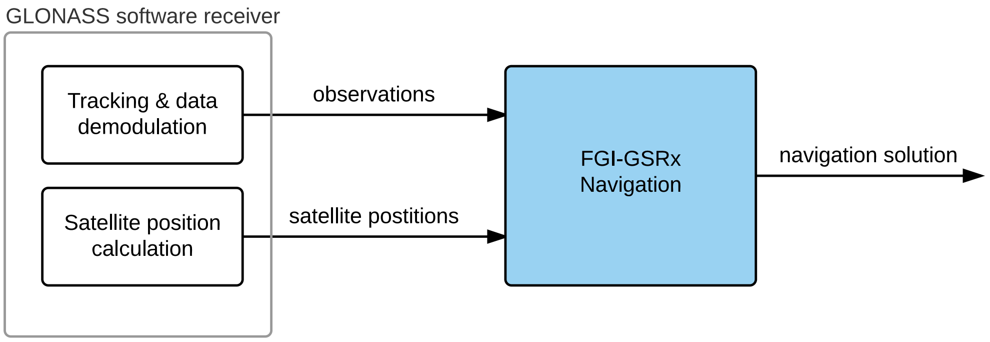
GLONASS software receiver
Tracking & data demodulation
Satellite position calculation
observations
satellite postitions
FGI-GSRx Navigation
navigation solution

Figure 15: GLONASS navigation solution flow. Pseudorange observations and satellite positions are extracted from the incoming signals, and used by the navigation function to calculate a solution.

The observables are corrected by the satellite clock corrections and atmospheric corrections. The satellite clock corrections in GLONASS and GPS have different sign conventions, which should be taken into account in the combined use of the systems. In FGI-GSRx the GLONASS clock corrections are stored with the sign of the $\tau_n(t_b)$ parameter inverted, so they can be used like the GPS corrections.

Once the inputs of the navigation block, i.e., pseudorange measurements and satellite positions, are available, a navigation solution is calculated. The positioning calculation can use either a epoch-by-epoch least-squares method or a recursive Kalman filter method. Development of the position solution was not part of this thesis, as the navigation functions are already implemented in FGI-GSRx. The positioning solution using GLONASS was tested in order to verify the implemented GLONASS signal-specific functions. The test results are presented in Chapter 5.

4.7 Summary

This chapter presented the implementation of acquisition, tracking, data demodulation, and satellite position computation functions GLONASS signal processing in the FGI-GSRx receiver. GLONASS signals can be processed in parallel to GPS, Galileo and BeiDou. Main differences are in the satellite position calculations and carrier and code tracking. Acquisition functions were developed, tracking functions were modified for GLONASS, and data demodulation and satellite position calculation functions were developed. The matlab-files added to FGI-GSRx are listed in Table 8.

Table 8: GLONASS matlab-code files created, sorted by folder within the FGI-GSRx file structure.

Folder	Description	File name
acq\	Signal acquisition	gloAcquisition.m
bit\	Bit synchronization	gloBitSync.m
frame\	Data decoding	gloDecodeData.m gloDecodeEphemeris.m gloDecodeEphemerisString.m gloFindTimeMarks.m gloGetEphAndDecodeTow.m gloGetEphemerisString.m
mod\	Code generation	gloGenerateStCode.m gloMakeStTable.m
sat\	Satellite positions	gloSatpos.m
tracking\	Signal tracking	gloInitTracking.m gloNarrowWide.m gloSetChannelState.m gloUpdateChannelState.m

5 Verification and performance tests

This chapter presents the results of positioning performace tests of the GLONASS software-defined receiver implemented in Chapter 4. Positioning functionality is tested and preliminary positioning accuracy results are shown. In addition, the receiver is used to test the impact of a GPS jammer on multi-GNSS positioning.

5.1 Positioning performance

The positioning results were analyzed in order to verify the positioning calculation and the complete receiver software. The purpose of the tests was to verify that the receiver provides a positioning solution using GLONASS, as well as GPS.

The standalone GLONASS receiver was verified using a data set collected with the NSL Stereo front-end. To test combined GPS/GLONASS positioning, the data set was collected using both modules of the Stereo connected to an antenna via a signal splitter. The MAX2679b was configured to the GLONASS L1 frequency with the configuration shown in Table 6. The MAX2112 module was configured to the GPS L1 frequency and a bandwidth of 1.39 MHz. The duration of the data collection was 31 seconds. The positioning was performed using the LSE method. Default GPS ionospheric model corrections were applied to GLONASS measurements. Table 9 shows a statistical comparison of the positioning results using either GLONASS or GPS alone, or GPS and GLONASS combined, as well as the results using a narrower DLL early–late spacing. Shown are root mean square (RMS) errors of the horizontal and vertical components and number of satellites used. Mean position dilution of precision (PDOP) values are shown as a measure of the effect of satellite geometry on positioning. The ENU plots in Figures 16–20 show the east, north, and height components of the deviation from the true position as a function of time. The horizontal components of all of the positioning solutions are shown in Fig. 21.

The accuracy of GLONASS positioning is expected to be comparable to GPS. However, the experimental results show that noticeably more error was present the GLONASS positioning results. The effects of different coordinate reference frame transformations between WGS 84 and PZ-90 on positioning results were investigated, but the resulting differences were of the order of millimeters. As stated in Section 4.5, the orbit calculations were also verified to be correct.

It may be the case that more noise or multipath propagation effects were present in the GLONASS observables. A narrower early–late spacing can be used to reduce errors from multipath [41]. Modifications to the code tracking loop proved to help in improving the positioning accuracy. Namely, reducing the early–late spacing from 0.5 chips to 0.1 chips. The raw GLONASS data from the previous test was processed again with the tracking DLL set to use an early–late spacing 0.1 chips instead of the default 0.5 chips. For the GPS–only data, the same narrower correlator spacing did not improve the positioning results. This can be explained by the narrower bandwidth of the GPS front-end. As mentioned in [42], the early–late spacing Δ_{EL}

is limited by bandwidth (BW) and chipping rate f_c according to:

$$\Delta_{EL} \geq \frac{f_c}{BW}. \tag{27}$$

Therefore the GLONASS signal, which was received using a wider bandwidth due to the FDMA signal, benefits more from the narrower correlator spacing.

Table 9: Positioning results comparison between GLONASS, GPS and combined GPS+GLONASS. Signals was tracked alternatively with an E-L spacing of 0.5 chips and 0.1 chips.

Configuration	Δ_{EL}	Horizontal RMS	Vertical RMS	PDOP	Satellites
GPS	0.5	4.8 m	5.6 m	2.02	8
GLONASS	0.5	11.2 m	7.2 m	2.54	6
GLONASS	0.1	3.4 m	6.6 m	2.54	6
GPS+GLONASS	0.5	5.5 m	5.4 m	1.55	12
GPS+GLONASS	0.1	3.1 m	5.6 m	1.55	12

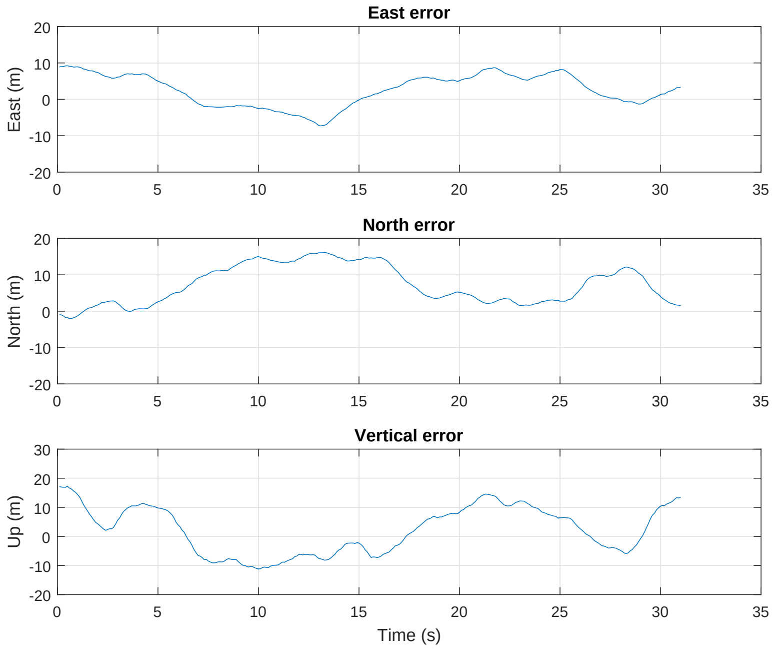

Figure 16: East, north and up components of positioning error using GLONASS with early-late spacing of 0.5 chips.

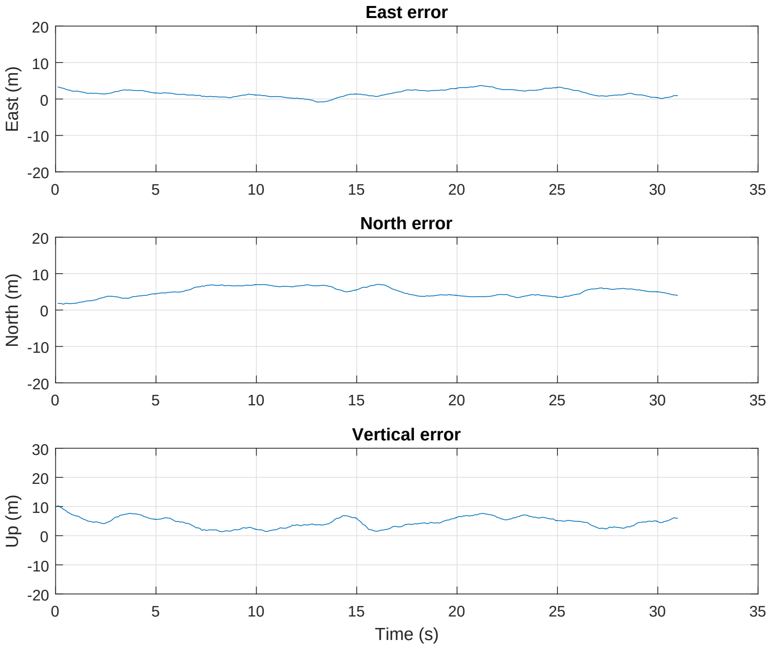

Figure 17: East, north and up components of positioning error using GLONASS with early-late spacing of 0.1 chips.

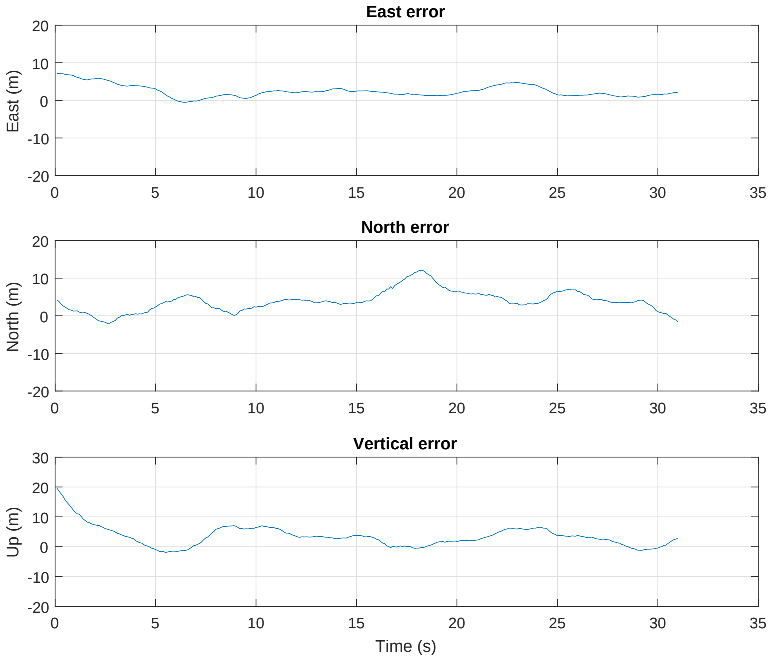

Figure 18: East, north and up components of positioning error using GPS with early-late spacing of 0.5 chips.

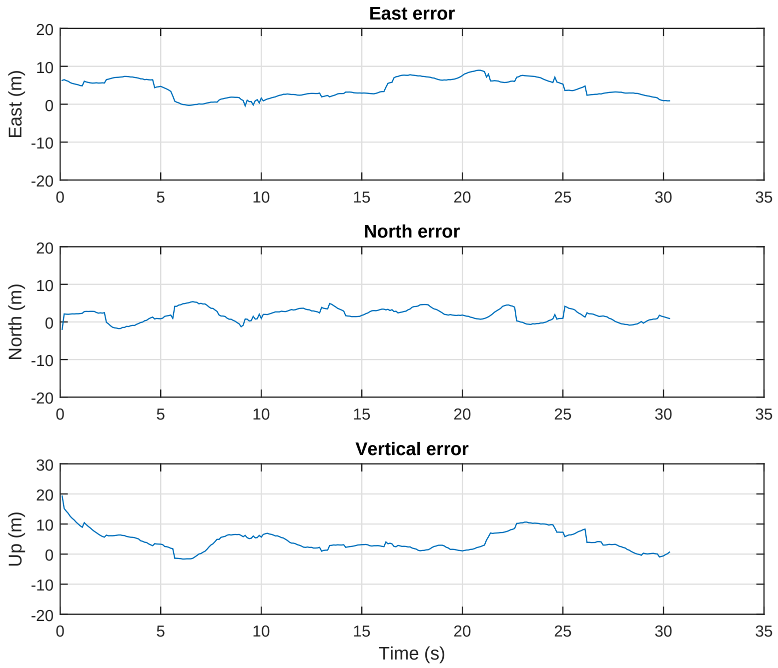

Figure 19: East, north and up components of positioning error using GLONASS and GPS with early-late spacing of 0.5 chips.

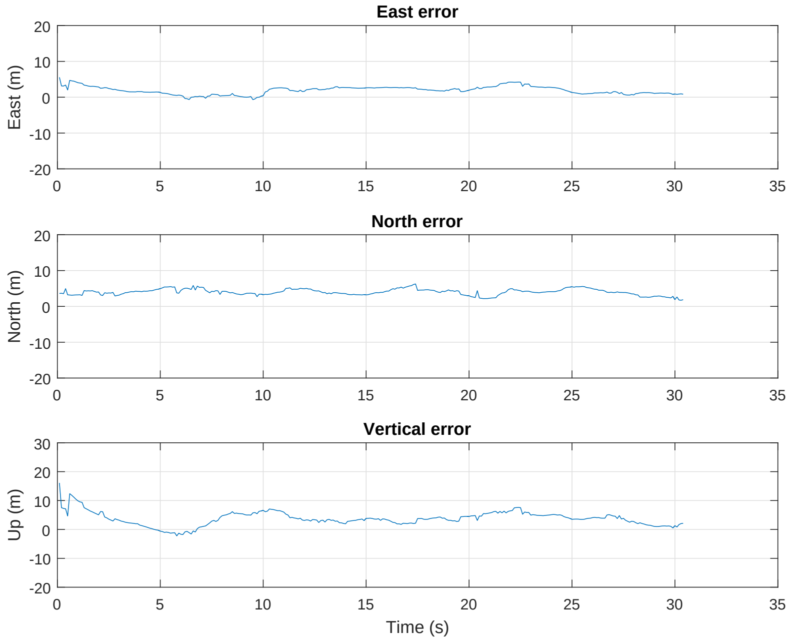

Figure 20: East, north and up components of positioning error using GLONASS and GPS with early-late spacing of 0.1 chips.

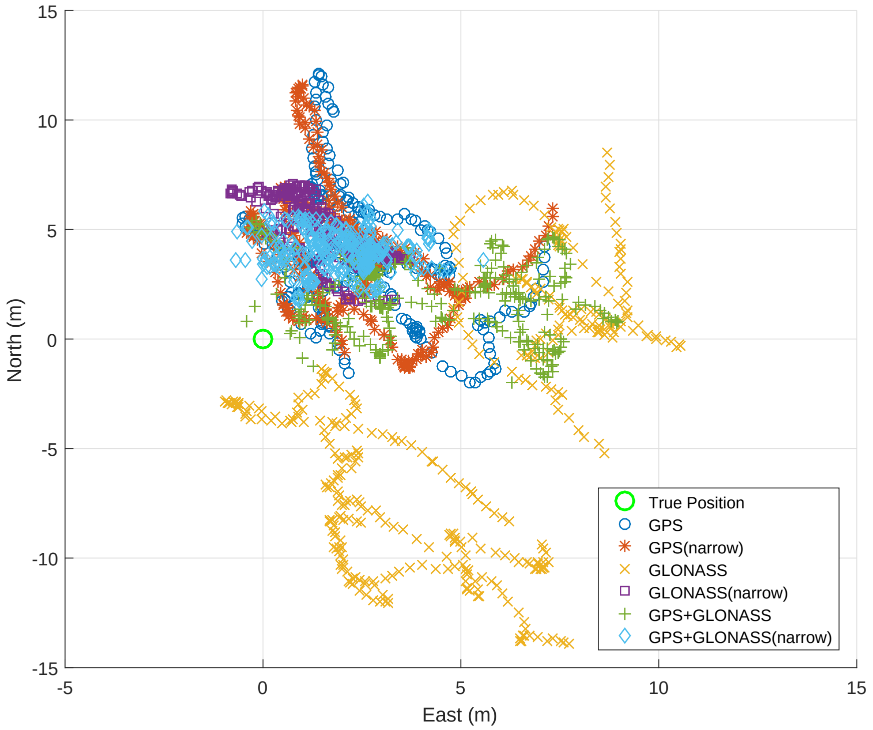

Figure 21: Scatter plot of the horizontal position errors of each positioning solution with reference to the true position, over 31 seconds at 100 ms intervals.

5.2 Effects of a cheap commercial jammer on multi-GNSS positioning

One of the aims of implementing the multi-constellation software receiver was to investigate the effects of interference on multi-GNSS positioning. Since the received power of GNSS signals is very weak, they are susceptible to interference. Hostile and intentional interference is known as jamming. Cheap, portable jamming devices are available on the market as "personal privacy devices" (PPDs), even though their use is illegal. Such devices have been reported to cause problems to GNSS users [43].

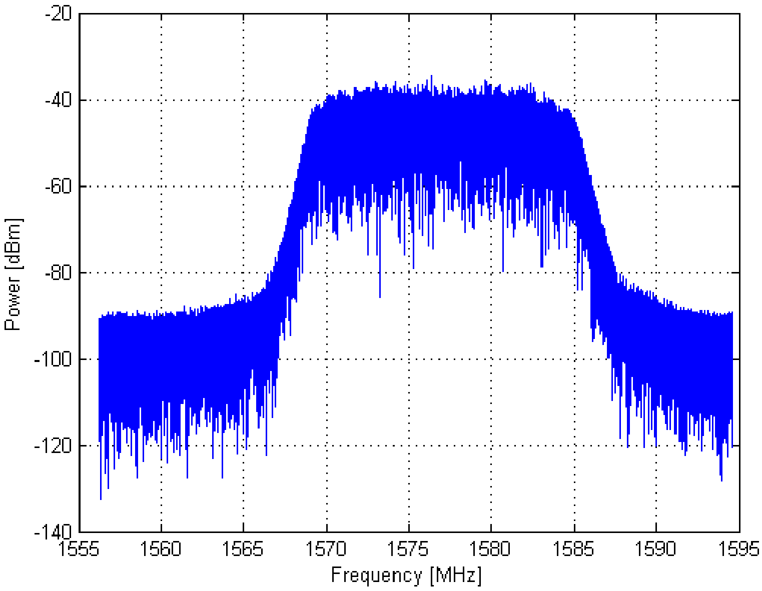

Figure 22: Power spectrum of the GPS L1 jammer.

The effect of jamming on combined GPS, GLONASS, and BeiDou positioning was tested in an experiment using the software receiver, a GNSS signal repeater and a commercial GPS L1 jammer [44]. The jammer transmits a 'chirp' signal, i.e., it rapidly sweeps across a range of frequencies. It has a center frequency of 1.577 GHz and a 3-dB bandwidth of 16 MHz. The power spectrum is shown in Fig. 22. The jammer was operated at a low power level inside the laboratory of FGI. A special permission required to operate the jammer was granted by the Finnish Communications Regulatory Authority (Viestintävirasto), allowing to operate the jammer in the FGI premises with a maximum power of –30 dBm.

Two NSL Stereo front-ends were used to capture the GNSS signals. One Stereo was configured to receive GPS L1 with Maxim 2769B and BeiDou B1 with Maxim 2112. A second NSL Stereo was configured to receive GLONASS with Maxim 2769B and BeiDou B2 with Maxim 2112.

The raw signal samples from the two Stereo front-ends were collected using two laptops. The signals were received with a multi-frequency GNSS antenna. GNSS signals were transmitted indoors using a GNSS signal repeater. The test setup is

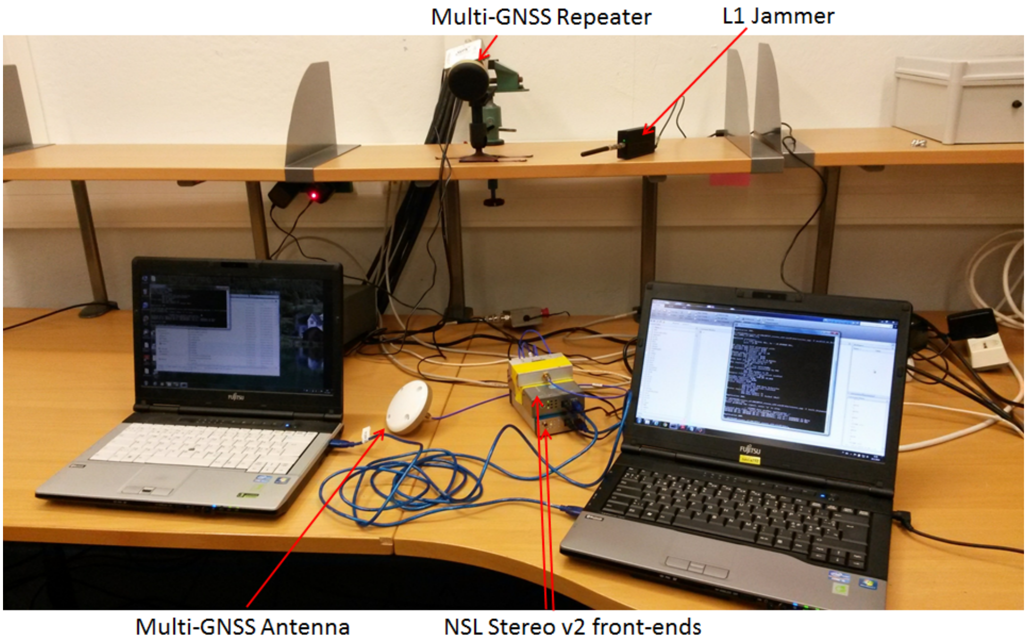

Figure 23: Test setup with multi-GNSS front-ends and L1 jammer [44].

shown in Fig. 23. The signals were collected for 120 seconds. The jammer was switched on after 65 seconds.

A jamming detection method based on Running Digital Sum (RDS) check of the digitized signal was tested. The method was first presented in [21]. Further details on the improved method tested here are given in [44].

C/N_0 plots showing the effects of jamming on each signal are shown in Figures 24–27. As is expected, the GPS L1 signal is the most affected by the L1 jammer. GLONASS is less affected, however more than BeiDou B1. The B2 signal at 1207.14 MHz, which is sufficiently far from the L1 frequency, is unaffected by the L1 jammer. The spectrum plots of the received signals in Fig. 28 illustrate that the jammer causes interference also in the GLONASS and BeiDou B1 bands.

GPS positioning performance was most affected by the presence of the L1 jammer, followed by GLONASS L1 and BeiDou B1. Multi-GNSS positioning solution is severely degraded by L1 jamming, as can be seen from the positioning errors in Fig. 29. When a jamming detection based constellation selection applied, as in Fig. 30, the multi-GNSS performance is improved. In this case, when jamming was detected on the L1 frequency, the navigation process switched to a single-frequency BeiDou B2 solution.

The results show how multi-constellation positioning solution is more robust against jamming. The effects of jamming in the GPS L1 frequency can be mitigated using a jamming detection based multi-GNSS constellation selection approach.

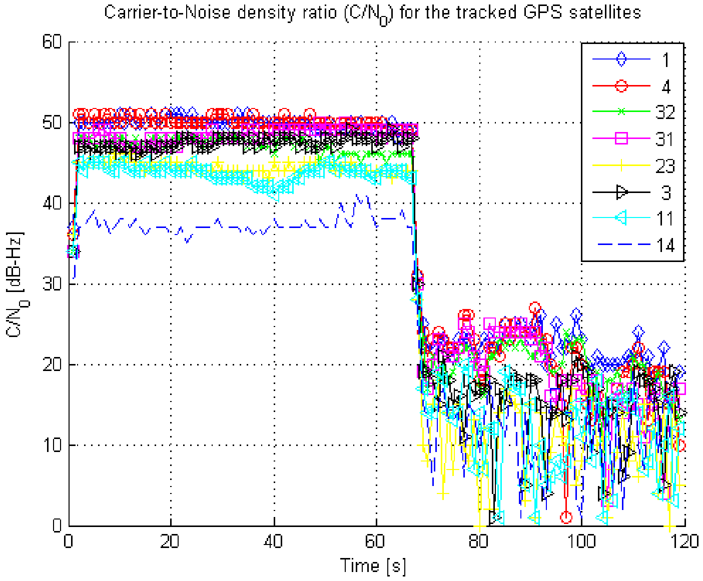

Figure 24: Carrier-to-noise density ratios for GPS signals during jamming test [44]. Satellite identifier numbers are shown in the legend.

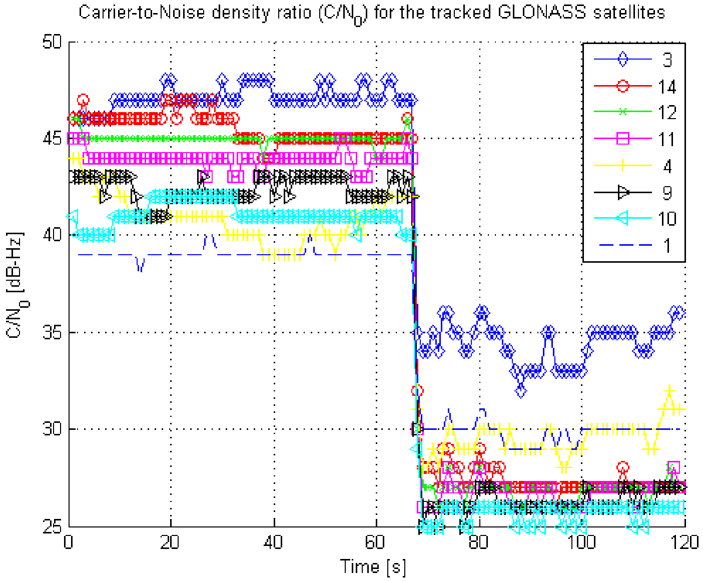

Figure 25: Carrier-to-noise density ratios for GLONASS signals during jamming test [44]. Satellite identifier numbers are shown in the legend.

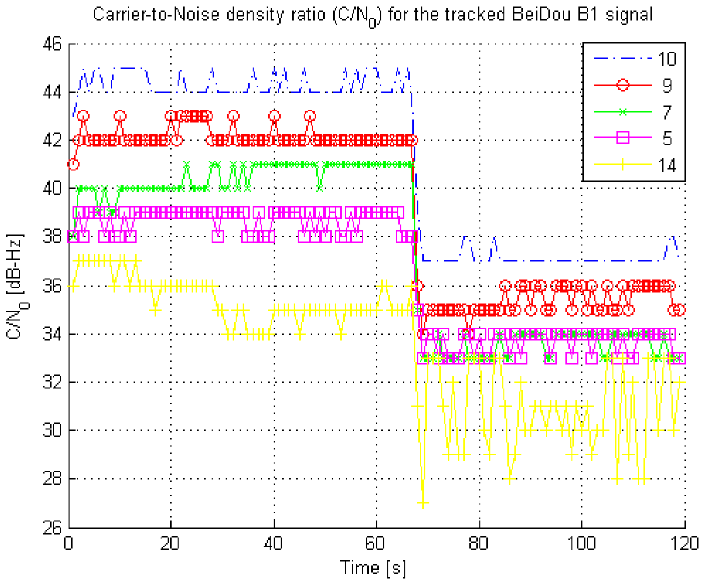

Figure 26: Carrier-to-noise density ratios for BeiDou B1 signals during jamming test [44]. Satellite identifier numbers are shown in the legend.

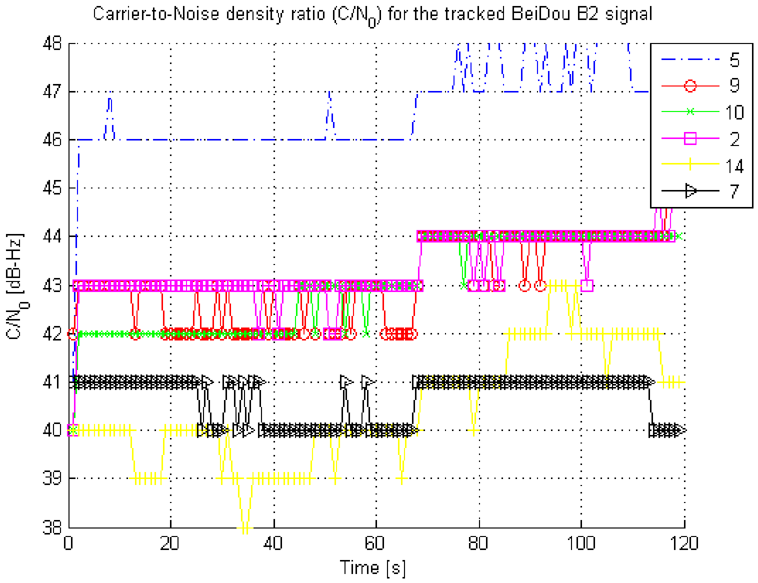

Figure 27: Carrier-to-noise density ratios for BeiDou B2 signals during jamming test [44]. Satellite identifier numbers are shown in the legend.

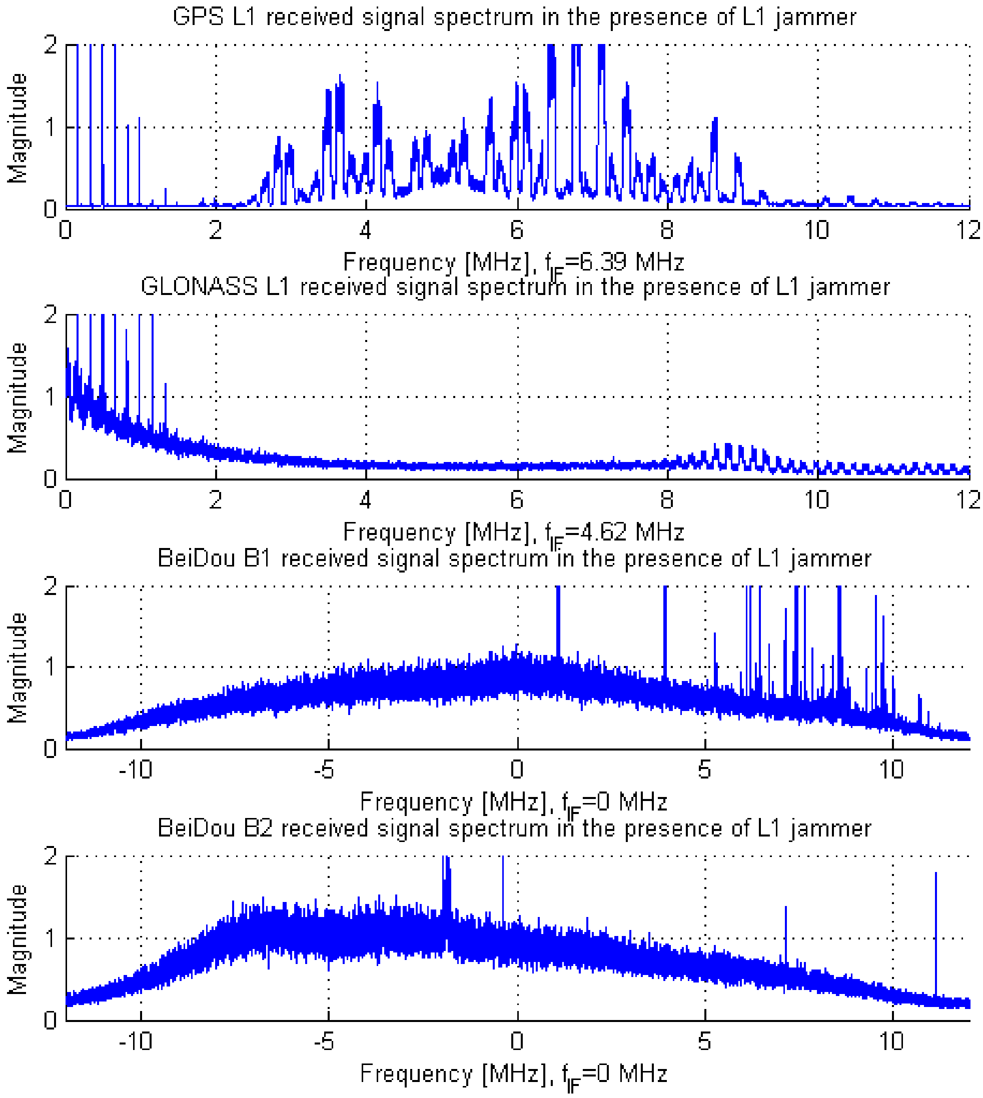

Figure 28: Multi-GNSS signal spectrum in the presence of L1 jammer [44].

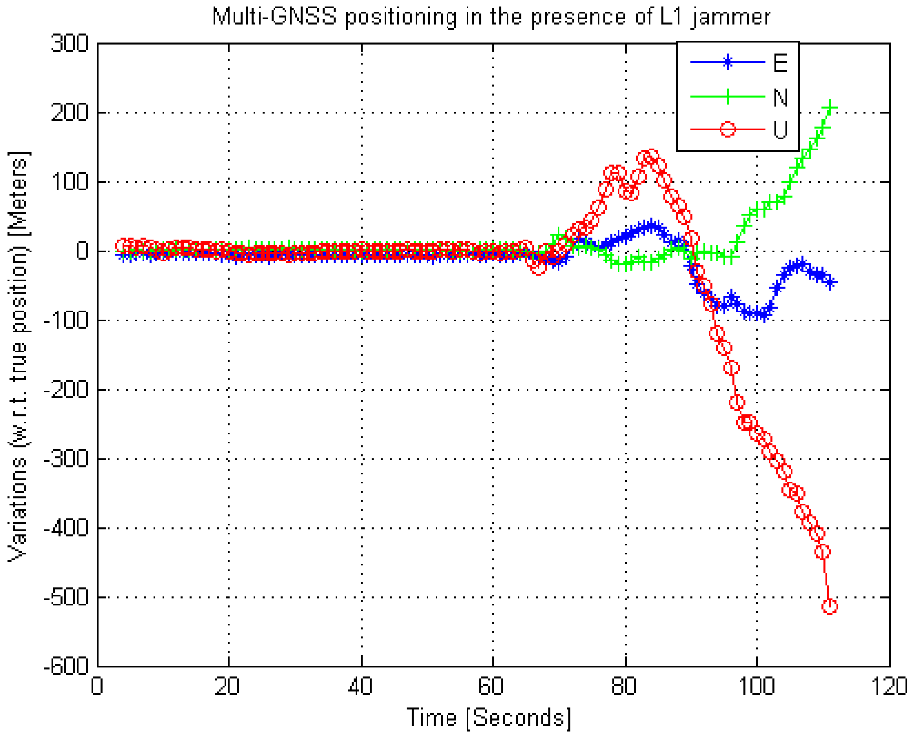

Figure 29: Multi-GNSS positioning errors in east-north-up (ENU) frame in the presence of L1 jammer [44].

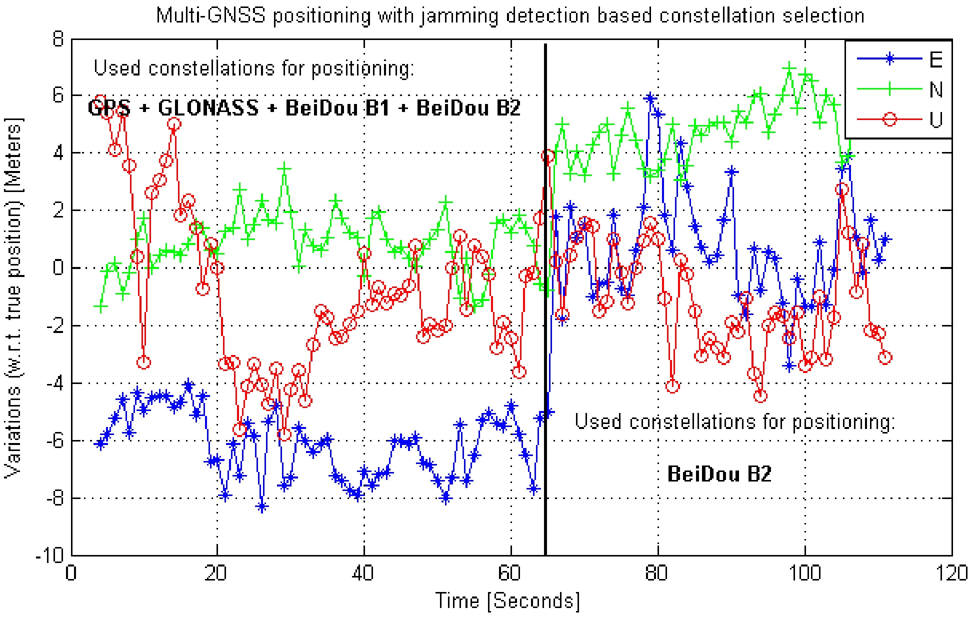

Figure 30: Multi-GNSS positioning errors in east-north-up (ENU) frame with jamming detection based GNSS selection [44].

6 Conclusions

The aim of this thesis was to implement GLONASS L1 capability in a multi-frequency, multi-GNSS software-defined receiver. The GLONASS signal capability was added to the FGI-GSRx receiver, which previously had GPS, Galileo, BeiDou, and IRNSS support.

The goals were for the receiver to be able to process GLONASS signals received using a suitably configured front-end, produce pseudorange measurements and satellite coordinates, and navigate using GLONASS signals alone, or in combination with other signals. The goals were met, and the software receiver can now be used to process signals from any of the above mentioned satellite navigation systems.

Software functions were developed for FGI-GSRx that allow GLONASS signals to be processed in parallel to GPS, Galileo, BeiDou, and IRNSS. Acquisition functions were developed and tracking functions were modified for GLONASS. Data demodulation and satellite position calculation functions were implemented.

Functional tests were performed, and tests of the positioning accuracy showed a slightly larger mean error in GLONASS positioning compared to GPS. GLONASS accuracy was improved by applying a narrower DLL discriminator.

The implemented software was applied in an analysis of the benefits of multi-GNSS positioning in the presence of jamming. The results of this analysis were presented at the 2015 International Association of Institutes of Navigation (IAIN) World Congress [44]. These tests showed that including GLONASS in the positioning solution offers benefits such as an increased number of measurements and better resilience against jamming. However, an optimum selection of the satellites is important in order to maximize the accuracy of the positioning solution.

In future development, the sensitivity of the GLONASS tracking could be improved by lengthening the integration time after bit synchronization. This would be facilitated by implementing lock detectors for the carrier and code tracking loops. Another feasible addition would be support for the GLONASS L2 signal, which is similar to the L1 signal.

In the implementation of the software, it became apparent that compared to the GPS, Galileo, and BeiDou signals, implementing GLONASS in a multi-constellation receiver creates more complexity in the receiver. A greater number of specialized functions are needed due to differences in the signal and in the navigation message. These differences include the FDMA multiplexing and the format of the satellite position coordinates in the navigation data broadcast. However, a software receiver framework facilitates the adding of new signals. Finally, it can be said that the FGI-GSRx receiver is now a complete multi-constellation GNSS receiver.

References

[1] European GNSS Agency, *GNSS market report*. European Commission Publications Office, Mar. 2015.

[2] C. Fernandez-Prades, L. Lo Presti, and E. Falletti, "Satellite Radiolocalization From GPS to GNSS and Beyond: Novel Technologies and Applications for Civil Mass Market," *Proceedings of the IEEE*, vol. 99, no. 11, pp. 1882–1904, Nov. 2011.

[3] J. T. Curran, M. Petovello, and G. Lachapelle, "Design Paradigms for Multi-Constellation Multi-Frequency Software GNSS Receivers," in *China Satellite Navigation Conference (CSNC) 2013 Proceedings*, ser. Lecture Notes in Electrical Engineering, J. Sun, W. Jiao, H. Wu, and C. Shi, Eds. Springer Berlin Heidelberg, 2013, vol. 243, pp. 751–765.

[4] C. Fernandez-Prades, J. Arribas, L. Esteve, D. Pubill, and P. Closas, "An open source galileo E1 software receiver," in *Satellite Navigation Technologies and European Workshop on GNSS Signals and Signal Processing,(NAVITEC), 2012 6th ESA Workshop on*. IEEE, 2012.

[5] J. Mitola, "The software radio architecture," *IEEE Communications Magazine*, vol. 33, no. 5, pp. 26–38, May 1995.

[6] Y. Urlichich, V. Subbotin, G. Stupak, V. Dvorkin, A. Povalyaev, and S. Karutin, "GLONASS Modernization," in *Proceedings of the 24th International Technical Meeting of The Satellite Division of the Institute of Navigation (ION GNSS 2011)*, Portland, OR, Sep. 2011, pp. 3125–3128.

[7] E. D. Kaplan, J. L. Leva, D. Milbert, and M. S. Pavloff, "Fundamentals of Satellite Navigation," in *Understanding GPS: Principles and Applications*, 2nd ed., E. D. Kaplan and C. Hegarty, Eds. Norwood, MA: Artech House, 2005.

[8] B. W. Parkinson and J. J. Spilker, Jr., *Global Positioning System: Theory and Applications*. American Institute of Aeronautics & Astronautics, 1996.

[9] R. Conely, R. Cosentino, C. Hegarty, E. D. Kaplan, J. L. Leva, M. Uijt de Haag, and K. Van Dyke, "Performance of Stand-Alone GPS," in *Understanding GPS: Principles and Applications*, 2nd ed., E. D. Kaplan and C. Hegarty, Eds. Norwood, MA: Artech House, Nov. 2005.

[10] P. W. Ward, J. W. Betz, and C. Hegarty, "Satellite Signal Aqcuisition, Tracking, and Data Demodulation," in *Understanding GPS: Principles and Applications*, 2nd ed., E. D. Kaplan and C. Hegarty, Eds. Norwood, MA: Artech House, 2005.

[11] K. Borre, D. M. Akos, N. Bertelsen, P. Rinder, and S. H. Jensen, *A Software-Defined GPS and Galileo Receiver: A Single-Frequency Approach*. Boston, MA: Birkhäuser, 2006.

[12] A. Brown, M. May, and B. Tanju, "Benefits of Software GPS Receivers for Enhanced Signal Processing," *GPS Solutions*, vol. 4, no. 1, pp. 56–66, Jul. 2000.

[13] P. W. Ward, J. W. Betz, and C. Hegarty, "GPS Satellite Signal Characteristics," in *Understanding GPS: Principles and Applications*, 2nd ed., E. D. Kaplan and C. Hegarty, Eds. Norwood, MA: Artech House, 2005.

[14] Russian Space Systems, "Global Navigation Satellite System GLONASS - Interface Control Document," Feb. 2014. [Online]. Available: http://www.spacecorp.ru/directions/glonass/control_document/

[15] M. S. Grewal and A. P. Andrews, *Kalman Filtering: Theory and Practice Using MATLAB*, 3rd ed. Hoboken, NJ: Wiley & Sons, 2008.

[16] D. M. Akos, "A software radio approach to global navigation satellite system receiver design," Ph.D. Thesis, Ohio University, 1997.

[17] J. B.-Y. Tsui, *Fundamentals of Global Positioning System Receivers: A Software Approach*. Hoboken, NJ: Wiley & Sons, 2005.

[18] S. Gleason and D. Gebre-Egziabher, Eds., *GNSS Applications and Methods*, 1st ed. Norwood, MA: Artech House, 2012.

[19] A. Gavrilov, "GLONASS Receiver Written in Scilab," Sep. 2011, retrieved: February 26, 2015. [Online]. Available: http://gnss-sdr.ru/index.php?itemid=23

[20] B. Motella, M. Pini, and F. Dovis, "Investigation on the effect of strong out-of-band signals on global navigation satellite systems receivers," *GPS Solutions*, vol. 12, no. 2, pp. 77–86, Dec. 2007.

[21] M. Z. H. Bhuiyan, H. Kuusniemi, S. Söderholm, and E. Airos, "The Impact of Interference on GNSS Receiver Observables–A Running Digital Sum Based Simple Jammer Detector," *Radioengineering*, vol. 23, no. 3, 2014.

[22] C. H. Kang, S. Y. Kim, and C. G. Park, "A GNSS interference identification using an adaptive cascading IIR notch filter," *GPS Solutions*, vol. 18, no. 4, pp. 605–613, Dec. 2013.

[23] D. Borio, L. Camoriano, and L. Lo Presti, "Two-Pole and Multi-Pole Notch Filters: A Computationally Effective Solution for GNSS Interference Detection and Mitigation," *IEEE Systems Journal*, vol. 2, no. 1, pp. 38–47, Mar. 2008.

[24] Y.-H. Chen, J.-C. Juang, J. Seo, S. Lo, D. M. Akos, D. S. De Lorenzo, and P. Enge, "Design and Implementation of Real-Time Software Radio for Anti-Interference GPS/WAAS Sensors," *Sensors (Basel, Switzerland)*, vol. 12, no. 10, pp. 13 417–13 440, Oct. 2012.

[25] S. Abbasian Nik and M. G. Petovello, "Implementation of a Dual-Frequency GLONASS and GPS L1 C/A Software Receiver," *The Journal of Navigation*, vol. 63, no. 02, pp. 269–287, Apr. 2010.

[26] M. Anghileri, T. Pany, D. Sanroma-Güixens, J.-H. Won, A. Sicramaz-Ayaz, C. Stöber, I. Krämer, D. Dötterböck, G. W. Hein, and B. Eissfeller, "Performance evaluation of a multi–frequency GPS/Galileo/SBAS software receiver," in *Proceedings of the 20th International Technical Meeting of the Satellite Division of the Institute of Navigation (ION GNSS'07), Fort Worth, TX*, 2007, pp. 2749–2761.

[27] T. Paakki, J. Raasakka, F. Della Rosa, H. Hurskainen, and J. Nurmi, "TUT-GNSS - University Based Hardware/Software GNSS Receiver for Research Purposes," in *Ubiquitous Positioning Indoor Navigation and Location Based Service (UPINLBS) 2010*, Oct. 2010.

[28] D. Akopian and A. Soghoyan, "A LabVIEW-based fast prototyping software defined GPS receiver platform," in *2013 IEEE Global Conference on Signal and Information Processing (GlobalSIP)*, Dec. 2013, pp. 1230–1233.

[29] H. Hurskainen, J. Raasakka, T. Ahonen, and J. Nurmi, "Multicore Software-defined Radio Architecture for GNSS Receiver Signal Processing," *EURASIP Journal on Embedded Systems*, vol. 2009, pp. 3:1–3:10, Jan. 2009.

[30] M. Z. H. Bhuiyan and S. Söderholm, "Overcoming the Challenges of BeiDou Receiver Implementation," *Sensors*, no. 14, pp. 22 082–22 098, Nov. 2014.

[31] M. Z. H. Bhuiyan, S. Söderholm, S. Thombre, L. Ruotsalainen, and H. Kuusniemi, "Implementation of a Software-Defined BeiDou Receiver," in *China Satellite Navigation Conference (CSNC) 2014 Proceedings: Volume I*, ser. Lecture Notes in Electrical Engineering. Springer Berlin Heidelberg, 2014, vol. 303, pp. 751–762.

[32] M. Z. H. Bhuiyan, S. Söderholm, S. Thombre, L. Ruotsalainen, M. Kirkko-Jaakkola, and H. Kuusniemi, "Performance evaluation of carrier-to-noise density ratio estimation techniques for BeiDou Bl signal," in *Ubiquitous Positioning Indoor Navigation and Location Based Service (UPINLBS) 2014*, Nov. 2014, pp. 19–25.

[33] M. Z. H. Bhuiyan, S. Söderholm, S. Thombre, L. Ruotsalainen, and H. Kuusniemi, "Performance Analysis of a Dual-Frequency Software-Defined BeiDou Receiver with B1 and B2 Signals," in *China Satellite Navigation Conference (CSNC) 2015 Proceedings: Volume I*, ser. Lecture Notes in Electrical Engineering. Springer Berlin Heidelberg, 2015, vol. 340, pp. 827–839.

[34] S. Thombre, M. Z. H. Bhuiyan, S. Söderholm, M. Kirkko-Jaakkola, L. Ruotsalainen, and H. Kuusniemi, "A Software Multi-GNSS Receiver Implementation for the Indian Regional Navigation Satellite System," *IETE Journal of Research*, Oct. 2015.

[35] S. Feairheller and R. Clark, “Other Satellite Navigation Systems,” in *Understanding GPS: Principles and Applications*, 2nd ed., E. D. Kaplan and C. Hegarty, Eds. Norwood, MA: Artech House, Nov. 2005.

[36] A. Zueva, E. Novikov, D. Pleshakov, and I. Gusev, “System of Geodetic Parameters “Parametry Zemli 1990” PZ-90.11,” in *9th Meeting of the Internatonal Commitee on GNSS (ICG-9)*, Prague, Czech Republic, Nov. 2014. [Online]. Available: http://www.unoosa.org/pdf/icg/2014/wg/wgd7.pdf

[37] GPS World, “GLONASS-K1 Satellite Launched Nov. 30,” Jan. 2014. [Online]. Available: http://gpsworld.com/glonass-k1-satellite-launched-nov-30/

[38] Nottingham Scientific Ltd, “Stereo v2 datasheet,” retrieved: Dec. 1, 2015. [Online]. Available: http://www.nsl.eu.com/datasheets/stereo.pdf

[39] C.-H. Cheng, “Calculations for positioning with the Global Navigation Satellite System,” M.S. thesis, Ohio University, 1998.

[40] Y. Lin, H. Guo, and M. Yu, “A Comparison for GLONASS Satellite Coordinate Calculation,” in *International Conference on Information Engineering and Computer Science, 2009 (ICIECS 2009)*, Dec. 2009.

[41] P. W. Ward, J. W. Betz, and C. Hegarty, “Interference, Multipath, and Scintillation,” in *Understanding GPS: Principles and Applications*, 2nd ed., E. D. Kaplan and C. Hegarty, Eds. Norwood, MA: Artech House, 2005.

[42] M. Z. H. Bhuiyan and S. E. Lohan, “Multipath Mitigation Techniques for Satellite-Based Positioning Applications,” in *Global Navigation Satellite Systems: Signal, Theory and Applications*, S. Jin, Ed. InTech, Feb. 2012.

[43] S. Pullen and G. Gao, “GNSS Jamming in the Name of Privacy,” *Inside GNSS*, no. March/April, 2012. [Online]. Available: http://www.insidegnss.com/node/2976

[44] M. Z. H. Bhuiyan, S. Honkala, S. Söderholm, and H. Kuusniemi, “Performance Analysis of a Multi-GNSS receiver in the Presence of a Commercial Jammer,” in *2015 International Association of Institutes of Navigation World Congress*, Prague, Czech Republic, Oct. 2015.